

# Cortical Afferents of the Perirhinal, Postrhinal, and Entorhinal Cortices of the Rat

REBECCA D. BURWELL<sup>1\*</sup> AND DAVID G. AMARAL<sup>2</sup>

<sup>1</sup>Department of Psychology, Brown University, Box 1853, Providence, Rhode Island 02912

<sup>2</sup>Department of Psychiatry and Center for Neuroscience, The University of California, Davis, Davis, California 95616

## ABSTRACT

We have divided the cortical regions surrounding the rat hippocampus into three cytoarchitecturally discrete cortical regions, the perirhinal, the postrhinal, and the entorhinal cortices. These regions appear to be homologous to the monkey perirhinal, parahippocampal, and entorhinal cortices, respectively. The origin of cortical afferents to these regions is well-documented in the monkey but less is known about them in the rat. The present study investigated the origins of cortical input to the rat perirhinal (areas 35 and 36) and postrhinal cortices and the lateral and medial subdivisions of the entorhinal cortex (LEA and MEA) by placing injections of retrograde tracers at several locations within each region. For each experiment, the total numbers of retrogradely labeled cells (and cell densities) were estimated for 34 cortical regions. We found that the complement of cortical inputs differs for each of the five regions. Area 35 receives its heaviest input from entorhinal, piriform, and insular areas. Area 36 receives its heaviest projections from other temporal cortical regions such as ventral temporal association cortex. Area 36 also receives substantial input from insular and entorhinal areas. Whereas area 36 receives similar magnitudes of input from cortices subserving all sensory modalities, the heaviest projections to the postrhinal cortex originate in visual associational cortex and visuospatial areas such as the posterior parietal cortex. The cortical projections to the LEA are heavier than to the MEA and differ in origin. The LEA is primarily innervated by the perirhinal, insular, piriform, and postrhinal cortices. The MEA is primarily innervated by the piriform and postrhinal cortices, but also receives minor projections from retrosplenial, posterior parietal, and visual association areas. *J. Comp. Neurol.* 398:179–205, 1998. © 1998 Wiley-Liss, Inc.

**Indexing terms:** polysensory cortex; hippocampus; memory; spatial; retrograde

Since the landmark studies of the famous amnesic patient H.M., research on the neural basis of memory has focused on various structures in the medial temporal lobe (Scoville and Milner, 1957). Whereas earlier work emphasized the contribution of the hippocampus, and sometimes the amygdala, more recent emphasis has centered on the cortical regions that surround the hippocampus including the perirhinal, parahippocampal, and entorhinal cortices. The evidence now indicates that, in addition to providing the primary cortical input to the hippocampus, these regions make unique contributions to certain forms of memory. For example, damage limited to the perirhinal cortex is sufficient to cause memory deficits in visual object recognition (Meunier et al., 1993; Ramus et al., 1994; Wiig et al., 1996) and visual discrimination learning (Buckley and Gaffan, 1997; Myhrer and Wangen, 1996; Wiig et al., 1996). Selective lesions of the entorhinal cortex also affect

performance on memory tasks (Hunt et al., 1994; Leonard et al., 1995; Otto et al., 1991). Thus far, a specific memory function has not been identified for the parahippocampal cortex, but studies in humans and monkeys suggest a possible role in the processing of spatial information (Aquirre et al., 1996; Habib and Sirigu, 1987; Malkova and Mishkin, 1997; Rolls and O'Mara, 1995). It is clear that the cortical regions surrounding the hippocampus are involved in memory functions, but their particular contributions and their functional interrelationships are not fully understood.

Grant sponsor: NIH; Grant number: NS 16980; Grant sponsor: NIMH; Grant number: F32-NS09247.

\*Correspondence to: Rebecca D. Burwell, Ph.D., Department of Psychology, Brown University, Box 1853, Providence, RI 02912.  
E-mail: Rebecca\_Burwell@Brown.edu

Received 28 November 1997; Revised 2 April 1998; Accepted 14 April 1998

The neuroanatomy of the monkey perirhinal, parahippocampal, and entorhinal cortices has been extensively examined (e.g., see Amaral et al., 1987; Jones and Powell, 1970; Suzuki and Amaral, 1994a,b; Van Hoesen and Pandya, 1972; Witter and Amaral, 1991; Witter et al., 1989). Much less is known, however, about these regions in the rat. Only a single study has comprehensively examined the afferents of the rat entorhinal cortex and that one largely ignored cortical afferents (Beckstead, 1978). There is also only a single comprehensive study of the cortical inputs to the rat perirhinal cortex (Deacon et al., 1983). Both of these studies, however, were based on areal boundaries that have now undergone revision. We recently proposed that the perirhinal cortex in the rat be divided into two regions: a rostral region that bears cytoarchitectonic and connectional similarities to the monkey perirhinal cortex, and a caudal portion, the postrhinal cortex, that is similar connectionally to the monkey parahippocampal cortex (Fig. 1; Burwell et al., 1995). The evidence now indicates that the perirhinal and postrhinal cortices project preferentially to different portions of the entorhinal cortex (Burwell and Amaral, 1998; Naber et al., 1997). These findings highlight the importance of describing the topography of the cortical afferents of these regions. The goal of the present series of studies was to provide a comprehensive and quantitative assessment of the cortical inputs to the entorhinal, perirhinal, and postrhinal cortices by using modern tract tracing techniques and rigorous quantification of neuroanatomical material. Our goal was to conduct studies in the rat that would provide data similar to those that were previously acquired for the monkey brain (Insauti et al., 1987; Suzuki and Amaral, 1994a). These data would hopefully foster comparisons of the functional organization of these memory-related brain regions in two common animal models of human memory.

## MATERIALS AND METHODS

### Subjects

Subjects were 46 previously untreated male Sprague-Dawley rats (Harlan Laboratories, Houston, TX) weighing

between 300 and 400 g. The brains of 20 subjects, those containing the 37 successful injection sites listed in Table 1, were selected for more detailed analysis. Data on connections between the perirhinal, postrhinal, and entorhinal cortices from these cases have been previously described (Burwell and Amaral, 1998). Prior to surgery, all subjects were housed individually or in pairs under standard vivarium conditions with ad libitum access to food and water. Following surgery, subjects were housed individually. All methods involving the use of live subjects were approved by the appropriate institutional animal care committee and conform to NIH guidelines.

### Surgery

One of two anesthesia protocols was used for each surgery; subjects were either injected with sodium pentobarbital ( $n = 17$ , Nembutal®, Abbott Laboratories, North Chicago, IL, 50 mg/kg, i.p.) or brought to a surgical level with halothane gas ( $n = 29$ ). A subject was then secured in a Kopf stereotaxic apparatus in the flat skull position. A hole was drilled into the skull above each intended injection site and a small incision was made in the dura to permit unobstructed penetration of the glass micropipette. After all injections were completed, the wound was sutured and the animals were kept warm in their cages for 1–2 hours before being returned to the colony.

The retrograde tracers, Fast Blue or Diamidino Yellow (FB, DY, Dr. Illing, GmbH and Co., Gross Umstadt, Germany), were injected at various locations within the perirhinal, postrhinal, and entorhinal cortices by using stereotaxic coordinates derived from Paxinos and Watson (1986). For FB, approximately 150 nl of a 3% solution in distilled H<sub>2</sub>O was injected. For DY, approximately 200 nl of a 2% solution in distilled H<sub>2</sub>O was injected. All but one subject received two retrograde tracer injections (FB and DY) and one anterograde tracer injection not relevant to the present study. The remaining subject, 108FG, received a single injection of 100 nl of a 2% solution of Fluoro-Gold (FG, Fluorochrome, Inc., Englewood, CO) in normal saline (Schmued and Fallon, 1986). The tracers were pressure-injected through glass micropipettes (tip diameters rang-

### Abbreviations

ACAd	dorsal anterior cingulate area	ORBvl	ventrolateral orbital area
ACAv	ventral anterior cingulate area	PaSub	parasubiculum
AId	dorsal agranular insular area	PBS	phosphate-buffered saline
Alv	ventral agranular insular area	Par2	parietal cortex, area 2
AIp	posterior agranular insular area	Pir	piriform cortex
AUD	primary auditory area	PL	prelimbic area
AUD <sub>v</sub>	ventral auditory area	PR	perirhinal cortex
AUDp	posterior auditory area	POR	postrhinal cortex
CA1, CA2,		PostSub	postsubiculum
CA3	CA fields of the hippocampus	PTLp	posterior parietal association areas
DG	dentate gyrus	rs	rhinal sulcus
DY	Diamidino yellow	RSPd	dorsal retrosplenial area
EC	entorhinal cortex	RSPv	ventral retrosplenial area
FB	Fast blue	SSp	primary somatosensory area
FG	Fluoro-Gold	SSs	supplementary somatosensory area
GU	gustatory area	Te <sub>v</sub>	ventral temporal association areas
HPC	hippocampus proper	Te <sub>2</sub>	temporal cortex, area 2
ILA	infralimbic area	Te <sub>3</sub>	temporal cortex, area 3
LEA	lateral entorhinal area	TH	area TH of parahippocampal cortex
MEA	medial entorhinal area	VISC	visceral area
MOs	secondary motor areas	VISl	lateral visual areas
MOp	primary motor area	VISm	medial visual areas
OC24	occipital cortex, area 24	VISp	primary visual area
ORB1	lateral orbital area	Area 35, 35	area 35 of the perirhinal cortex
ORBm	medial orbital area	Area 36, 35	area 36 of the perirhinal cortex
ORBv	ventral orbital area		

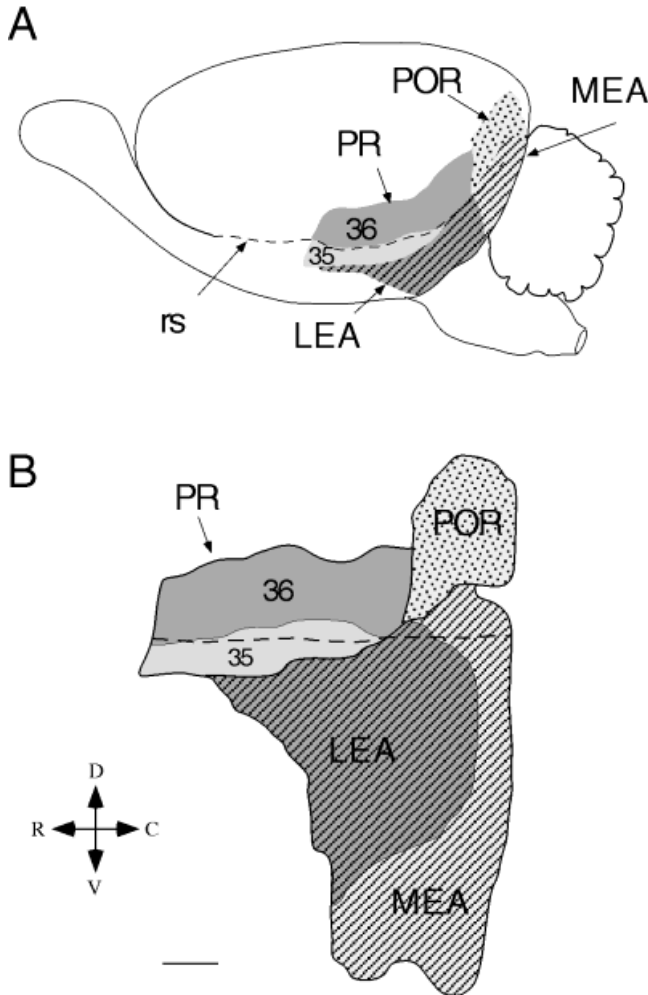


Fig. 1. **A:** Lateral view of the rat brain. The perirhinal cortex (PR) is shown in gray. The darker gray represents area 36 (36) and the lighter gray represents area 35 (35). The postrhinal cortex (POR) is indicated by a mottled shading pattern. The entorhinal cortex (EC) is shown in a hatched pattern. The lateral entorhinal area (LEA) is dark and the medial entorhinal area (MEA) is light. **B:** Unfolded surface map of the PR, POR, and EC with the same shading patterns. c, caudal; d, dorsal; r, rostral; rs, rhinal sulcus; v, ventral. Scale bar = 1 mm.

ing from 60 to 90  $\mu\text{m}$ ; Amaral and Price, 1983). The approximate rate of injection was 30 nl/minute. Following injection of the tracer, the micropipette was raised 100  $\mu\text{m}$ . After a 10-minute wait, the micropipette was slowly raised at a rate of approximately 500  $\mu\text{m}/\text{minute}$ .

### Tissue processing

Following a 7- to 9-day survival period, subjects were deeply anesthetized with a 35% solution of chloral hydrate and transcardially perfused by using a pH-shift protocol. Room temperature saline was first perfused for 2 minutes to clear the blood followed by a solution of 4% paraformaldehyde in 0.1 M sodium acetate buffer (pH 6.5) at 4°C for 10 minutes and of 4% paraformaldehyde in 0.1 M sodium borate buffer (pH 9.5) at 4°C for 15 minutes. Solutions were perfused at a flow rate of 35–40 ml/minute. Ice was packed around the head of the animals during perfusion. After removal from the skull, the brains were postfixed for

TABLE 1. Retrograde Tracer Injection Sites<sup>1,4</sup>

Location of injection	Experiment	Layer	Size (cu mm)
<b>Perirhinal</b>			
Rostral area 36	119FB	I–V	.08
Rostradorsal area 36	120FB	III–V	.11
Rostrventral area 36	97DY	III–V	.06
Midrostromcaudal area 36	98DY	I–V	.11
Midrostromcaudal area 36	132DY	V	.02
Midrostromcaudal area 36	94FB	V	.02
Ventral area 36	99DY	II–III	.06
Caudodorsal area 36	120DY	V	.02
Caudoventral area 36	100DY	V	.01
Rostral area 35	102DY	I–III	.06
Rostrventral area 35	132FB <sup>2</sup>	I–II	.02
Ventral area 35	112DY	V	.10
Caudal area 35	108FG	I–VI	.24
<b>Postrhinal</b>			
Rostral POR	97FB	V	.16
Rostrventral POR	102FB	V	.02
Middle POR	98FB	I–VI	.13
Caudodorsal POR	100FB	I–V	.17
Caudal POR	95DY	III–VI	.13
Caudal POR	99FB	I–V	.13
<b>Entorhinal</b>			
Rostrlateral LEA	113FB	I–V	.19
Rostral LEA	124FB	I–VI	.32
Rostral LEA	129DY	III–V	.05
Caudolateral LEA	130FB	V–VI	.04
Caudal LEA	128DY	V	.04
Caudal LEA	105DY	V	.06
Caudomedial LEA	105FB <sup>3</sup>	III–VI	.02
Medial LEA	129FB	V–VI	.02
Lateral MEA	113DY	V	.05
Lateral MEA	118FB	III–VI	.13
Caudomedial MEA	124DY	I–III	.18
MEA at medial LEA border	119DY	I–II	.07
MEA at medial LEA border	106DY	II–VI	.10
MEA at medial LEA border	128FB	V	.06
<b>Control</b>			
Rostral Te <sub>v</sub>	109FB	I–V	.11
Midrostromcaudal Te <sub>v</sub>	122FB	V–VI	.05
Caudal Te <sub>v</sub>	109DY	V	.25
VISI	94DY	I–V	.02

<sup>1</sup>For each experiment the regional and laminar location of the injection site are shown in the first and third columns. Retrograde injection sites have the suffix DY, FB, or FG for Diamidino Yellow, Fast Blue, and Fluoro-Gold.

<sup>2</sup>The dye core and heavy necrosis of the injection site in experiment 132FB involved superficial layers, but moderate necrosis was observed in an arc that extended into the external capsule.

<sup>3</sup>Experiment 105FB may have slightly involved the underlying white matter.

<sup>4</sup>Abbreviations for this and subsequent tables are found in the Abbreviations list.

6 hours in the final fixative at 4°C and then cryoprotected for 24 hours using 20% glycerol in 0.02 M potassium phosphate-buffered saline (KPBS, pH 7.4) at 4°C. The brains were then frozen and immediately sectioned or stored at –70°C.

The brains were coronally sectioned at 30  $\mu\text{m}$  on a freezing microtome. Sections were collected in five series for processing and storage. One 1:5 series was collected into 0.1 M phosphate buffer for retrograde tracer procedures. One series was mounted and stained for Nissl staining with thionin. One series was collected in KPBS for immunohistochemical processing of the anterograde tracer. The remaining two series were collected and stored at –20°C in cryoprotectant tissue collecting solution consisting of 30% ethylene glycol and 20% glycerol in sodium phosphate buffer (pH 7.4).

As soon as possible on the same day of sectioning, sections to be analyzed for fluorescent retrogradely labeled cells were mounted onto gelatin-coated slides. The mounted tissue was dried for 2–4 hours in a vacuum dessicator at room temperature, dehydrated in 100% ethanol (2  $\times$  2 minutes), cleared in xylene (3  $\times$  2 minutes), and coverslipped with DPX. This technique improves visibility and retards fading of fluorescent dyes, preserving material for repeated inspection for at least 3 years.

### Data analysis

Sections from each experiment were initially surveyed for location of the injection site by using darkfield optics for unstained tissue or brightfield optics for Nissl-stained tissue. Cases with injection sites in one of the target fields were further examined by fluorescence microscopy to verify adequate transport of the tracer. The contour of the hemisphere and the distribution of fluorescently labeled cells were then plotted for a 1:10 series of sections throughout the perirhinal, postrhinal, and entorhinal cortices ipsilateral to the injection site. Approximately 42–48 sections per case were quantified in this way. Labeled cells were plotted at a total magnification of 100 $\times$  using a Nikon Optiphot-2 coupled to a computerized data collection system (NeuroLucida V1.5, MicroBrightfield, Inc., Burlington, VT). The contours and plotted cells were then printed at a magnification of 16 $\times$ . The plots were aligned to adjacent Nissl-stained sections using a Wild stereomicroscope in order to add cytoarchitectonic borders for a set of 34 cortical regions and to document the location of the injection sites. Borders were determined based on the cytoarchitectonic criteria cited below in the section on nomenclature. All subsequent analyses were conducted on the printed computer plots.

To obtain an accurate estimate of total numbers of retrogradely labeled cells in each cortical area we used the fractionator sampling method (Gundersen et al., 1988; West, 1993). The fundamental principle is that when it is not possible to count all the cells in an anatomical structure, some method of sampling must be devised to ensure that all parts of the structure have an equal probability of being sampled. In the fractionator method, a known fraction of the volume of a structure is sampled. Thus, multiplying the number of cells counted by the reciprocal of the fractional volume sampled gives an estimate of the total number of cells. A systematic random sampling procedure is devised so that the first sample is randomly chosen and then all subsequent samples are taken at predetermined intervals.

The sampling procedure used for the present study is illustrated schematically in Figure 2. The predetermined intervals can be thought of as steps in the  $x$  (mediolateral),  $y$  (dorsoventral), and  $z$  (rostrocaudal) planes. A sampling box (stippled) was constructed based on a fraction of each of these sample intervals. The dimensions of the sampling box can be thought of as  $x'$ ,  $y'$ , and  $z'$ . Thus, the known fractional volume of the structure would be  $x'y'z'/xyz$ . An estimate for the entire structure can be calculated by multiplying the results of the sampling procedure by the reciprocal of the fractional volume,  $xyz/x'y'z'$ . For the example shown in Figure 2, assume that  $x'$  is half of  $x$ ,  $y'$  is half of  $y$ , and every tenth section in the  $z$  plane is assessed. If  $x$ ,  $y$ , and  $z$  each are equal to 10, then the fractional volume is  $(5 \cdot 5 \cdot 1)/(10 \cdot 10 \cdot 10) = .025$ , or  $1/40$ , and the reciprocal is 40. Thus, if a total of 500 objects were counted in the stippled sampling boxes, then an estimate for the number in the entire structure is  $40 \cdot 500$ , or 20,000 objects.

In the present study, the  $z$  step was always 300  $\mu\text{m}$  and  $z'$  was always 30  $\mu\text{m}$  because labeled cells were plotted for a 1:10 series of 30- $\mu\text{m}$  sections. The  $x$  step size was always equal to the  $y$  step size, and the  $x'$  size was always equal to the  $y'$  size. Thus, the box defined by the  $xy$  steps and the sampling box were always a square. The  $x'$  and  $y'$  length was either the same as, half of, or one-third of the length of the  $x$  and  $y$  steps. Consequently, the area of the sampling box (Fig. 2, shaded) was either the same as, one-quarter of,

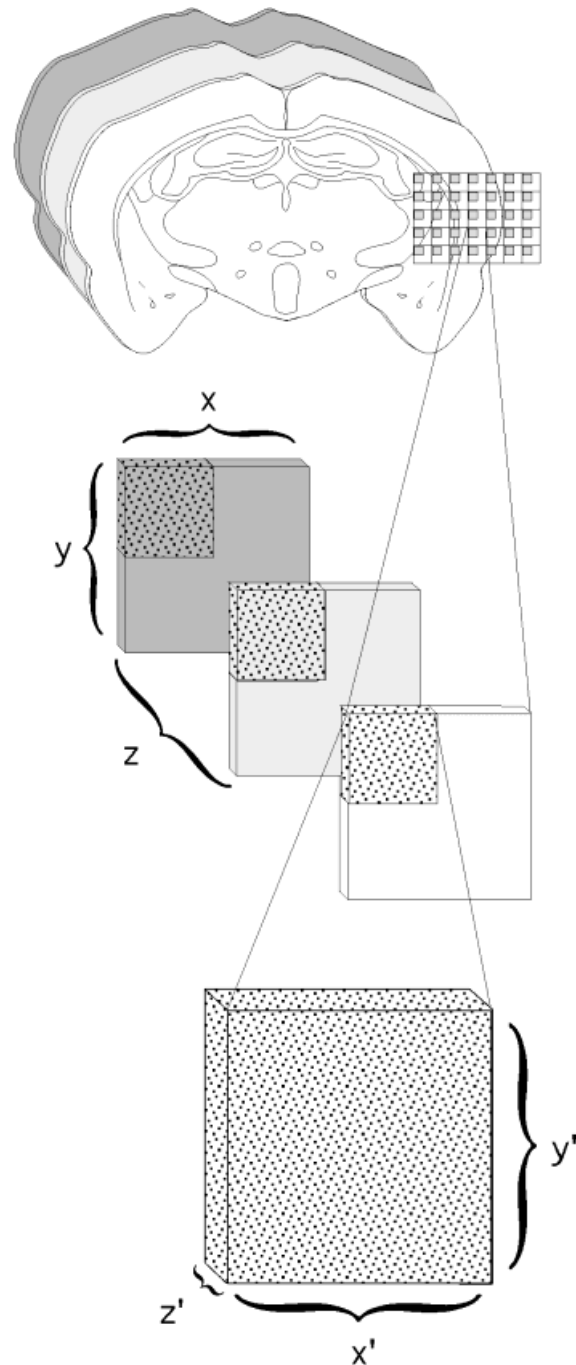


Fig. 2. Schematic showing the modified fractionator method used for estimating numbers of retrogradely labeled cells in the present study. See text for a more detailed account of the procedures. All the labeled cells in a known fraction of the cortical structure under analysis are counted. An estimate of the total cells in the structure is computed by multiplying the number of cells counted by the reciprocal of the fraction of the structure in which the counts were made. In the example shown in the schematic, the cortex is exhaustively sectioned and a subseries selected in which to count cells. A grid is placed over the structure to be quantified. In practice, of course, the grid is much finer. Only the cells located in the counting frames denoted by the stippled boxes for the selected sections are counted. In this example, the counting frames account for one-quarter of the total volume of a section. Thus, in this example, if all cells were counted in the stippled counting frames for a 1:10 series of sections,  $1/40$  of the total volume of the structure would have been quantified. Total labeled cells in the structure could be estimated by multiplying the number counted by 40 (the reciprocal of the fractional volume quantified).

or one-ninth of the area of the box formed by the  $xy$  steps. The same proportion would apply to the volume of tissue sampled as labeled cells were counted throughout the thickness of a section. The  $xy$  step size was selected based on the volume of the cortical region being sampled such that at least 100 samples were taken. The  $xy$  step size ranged from 200 to 600  $\mu\text{m}$ . The  $x'y'$  sample size was chosen based on the density of labeling and ranged from 150  $\mu\text{m}$  to 600  $\mu\text{m}$ . When density was relatively low, then  $x'y'$  length was made equal to the  $xy$  step size. In this case, all cells plotted in the structure were counted for a 1:10 series, or in  $1/10$  of the sections. This was the situation for the majority of the cortical regions sampled. When the density was higher, a fractional area of the structure per section was sampled, usually one-quarter. Figure 2 illustrates a sampling protocol in which the  $x'y'$  sampling box is half the  $xy$  step size. Thus, one-quarter of the coronal area would be sampled. On rare occasions, when the tissue was very densely labeled, one-ninth of the area in the coronal plane was sampled.

The specific protocol included the following steps: (1) the number of coronal sections containing portions of the cortical regions being sampled was assessed in order to choose an  $xy$  step size such that sampling frames totaled at least 100; (2) the density of labeling was assessed in order to determine the size of the sampling frame, larger frames for lower densities and smaller frames for higher densities; (3) a sampling template similar to the one shown in the upper panel of Figure 2 was placed randomly over the cortical region; (4) cells falling within the cortical region and entirely within a sampling frame were counted. Cells that fell on the lines bordering the left side and the bottom of the sampling frame were also counted. Cells that fell on the lines bordering the right side and the top of the sampling frame (the forbidden lines) were not counted; (5) the number of  $xy$  intersections (Fig. 2, arrow) falling within the cortical region was counted in order to estimate the area of the region for that section; and (6) when a portion of the injection site appeared on a coronal section plot, this area was quantified by counting the number of  $xy$  intersections falling within the region of dye deposit and the surrounding heavy necrosis.

For each cortical region, and each retrograde tracer injection, the following data were entered into a Microsoft Excel worksheet: the  $xy$  step size, the  $x'y'$  sample size, the number of  $xy$  intersections counted for each cortical section, and the number of cells counted for each cortical section. Entered on a summary worksheet was the number of  $xy$  intersections counted within the injection site for each cortical section on which the site appeared. From these data, the following estimates were calculated: the volume of the injection site, the volume of each cortical afferent region, the total numbers of cells labeled in each afferent region, the density of labeled cells in each afferent region in cells/cu mm, and the proportion of the estimated total labeled cells that fell within each afferent region. The proportions were based on the total number of labeled cells in the afferent regions and did not include any labeled cells in the region in which the injection site was located. For example, the proportions of labeled cells in each of the afferent regions for an injection site located in area 35 were calculated based on the total number of labeled cells in all regions except areas 35 and 36.

The fractionator sampling method that we have adapted for this study has certain strengths and limitations. One strength is that we were able to estimate both the total numbers of labeled cells in a region and the density of

labeled cells in a region. Having "forbidden lines" on two sides of the sampling frame was a strategy for ensuring that each cell has an equal probability of being counted in the  $xy$  plane. Given the way that we prepared this material, there was no way to correct for bias along the  $z$  axis, i.e., at the margins of coronal sections. The two likely sorts of bias along the  $z$  axis at the margins are increased probability of double counting and loss of caps (difficulty identifying partial cell bodies due to being sectioned at the margin of a coronal section). Whereas these two sorts of biases are likely to offset one another, there is still some bias in the sampling methods employed here. Nevertheless, estimates of cell number and density in all cortical regions were subject to the same bias and thus the relative densities and cell numbers should be accurate even if the absolute numbers are biased.

## RESULTS

We will first describe the nomenclature adopted for each of the cortical regions. This is then followed by descriptions of the injection sites. The pattern of input to the perirhinal, postrhinal, and entorhinal cortices is then described in three sections. Unless the topography and laminar patterns of the origins and/or terminations are similar across regional subdivisions, cortical afferents are described separately for perirhinal areas 36 and 35, and for entorhinal areas lateral entorhinal area (LEA) and medial entorhinal area (MEA). The patterns of input from the afferent regions are described in the order shown in Tables 2 and 3. In a final section, the patterns of cortical inputs to the perirhinal, postrhinal, and entorhinal regions are compared and contrasted.

### Nomenclature

Based on recent histochemical, connectional, and cytoarchitectonic criteria, we have proposed that the rat perirhinal cortex is divided into two regions, a rostral one for which we have retained the name perirhinal cortex, and a caudal one, that we call the postrhinal cortex (Burwell and Amaral, 1995; Burwell et al., 1995). These regions, together with the entorhinal cortex, occupy the lateral, ventral, and caudal surfaces of the posterior cortical mantle. The perirhinal and postrhinal cortices comprise a strip of cortex on the lateral surface of the rat brain with the perirhinal cortex lying rostral to the postrhinal cortex (Fig. 1, upper). The entorhinal cortex, which forms the ventral border for the posterior perirhinal cortex and the postrhinal cortex, wraps around the ventrocaudal surface of the brain (Fig. 1, lower). The perirhinal cortex occupies the fundus and both banks of the rostral portion of the posterior rhinal sulcus. The entorhinal cortex occupies the rhinal sulcus at caudal levels (Dolorfo and Amaral, 1993). The postrhinal cortex lies dorsally adjacent to the entorhinal cortex and does not include any of the cortex that lies within the rhinal sulcus. It should be noted that our definition of the postrhinal cortex differs from the one provided by Deacon et al. (1983).

A detailed description of the borders and neuroanatomical characteristics of the perirhinal and postrhinal regions is in preparation (Burwell and Amaral, unpublished observations). In the following paragraphs, we briefly describe the neuroanatomical features used to identify the borders of the perirhinal, postrhinal, and entorhinal cortices. The borders and nomenclature for other cortical regions are adapted from the atlases of Paxinos and Watson (1986) and Swanson (1992). Lateral and medial surface views of

TABLE 2. Percentages of Total Input to Target Regions<sup>1</sup>

Afferent regions	Target regions				
	Area 36	Area 35	POR	LEA	MEA
Piriform	5.6 ± 1.72	25.6 ± 4.24	0.2 ± 0.08	33.9 ± 6.83	30.7 ± 14.84
MOS	2.6 ± 0.79	3.3 ± 0.80	2.2 ± 0.26	1.8 ± 0.61	6.5 ± 4.05
MOp	0.8 ± 0.36	0.8 ± 0.26	0.4 ± 0.11	0.4 ± 0.17	0.8 ± 0.29
PL	0.5 ± 0.17	0.6 ± 0.24	0.1 ± 0.02	1.3 ± 0.21	0.4 ± 0.12
ILA	0.7 ± 0.24	0.5 ± 0.18	0.1 ± 0.03	1.7 ± 0.52	0.6 ± 0.36
ORBm	0.9 ± 0.18	0.5 ± 0.17	0.1 ± 0.03	1.7 ± 0.25	0.3 ± 0.15
ORB1	1.0 ± 0.56	1.5 ± 0.20	0.1 ± 0.03	1.4 ± 0.48	0.4 ± 0.17
ORBvl	1.1 ± 0.28	1.3 ± 0.33	0.7 ± 0.12	2.4 ± 0.46	1.0 ± 0.43
Frontal	7.6 ± 1.77	8.5 ± 1.87	3.6 ± 0.18	10.7 ± 1.22	10.0 ± 3.92
Ald	2.8 ± 0.79	5.0 ± 1.24	0.3 ± 0.08	6.3 ± 0.95	1.2 ± 0.46
Alv	4.3 ± 1.95	3.3 ± 0.62	0.1 ± 0.04	3.8 ± 0.28	1.4 ± 0.58
Alp	2.8 ± 0.99	7.6 ± 1.33	0.2 ± 0.05	8.4 ± 2.11	2.1 ± 0.83
GU	0.5 ± 0.19	1.5 ± 0.23	0.1 ± 0.04	1.1 ± 0.18	0.3 ± 0.12
VISC	2.4 ± 0.87	4.8 ± 0.93	0.3 ± 0.20	1.7 ± 0.45	0.9 ± 0.39
Insular	12.8 ± 2.85	22.2 ± 1.32	0.9 ± 0.27	21.2 ± 2.62	5.8 ± 1.84
AUD	4.6 ± 1.28	1.5 ± 0.97	2.8 ± 0.47	2.1 ± 1.12	1.0 ± 0.32
AUDv	4.1 ± 1.27	2.2 ± 1.55	0.6 ± 0.14	0.3 ± 0.14	0.3 ± 0.11
Area 35			0.9 ± 0.18	6.8 ± 0.99	1.6 ± 0.47
Area 36			7.4 ± 1.82	8.8 ± 1.69	5.5 ± 1.53
TeV	30.4 ± 4.18	7.3 ± 0.71	16.3 ± 3.69	3.0 ± 0.00	5.6 ± 0.00
POR	10.5 ± 3.19	1.7 ± 0.88		4.9 ± 0.97	7.1 ± 1.98
Temporal	49.7 ± 7.70	12.7 ± 5.54	27.9 ± 3.07	25.9 ± 4.05	21.1 ± 4.64
ACAd	0.4 ± 0.10	0.3 ± 0.11	1.0 ± 0.21	0.8 ± 0.26	1.7 ± 0.88
ACAv	0.0 ± 0.02	0.0 ± 0.02	0.1 ± 0.04	0.3 ± 0.20	0.5 ± 0.10
RSPd	1.2 ± 0.33	0.2 ± 0.07	10.6 ± 2.01	1.4 ± 0.68	5.8 ± 2.41
RSPv	0.1 ± 0.03	0.0 ± 0.01	1.8 ± 0.36	0.6 ± 0.46	3.2 ± 1.33
Cingulate	1.7 ± 0.33	0.6 ± 0.21	13.5 ± 2.20	3.1 ± 1.45	11.2 ± 3.79
LEA	10.1 ± 4.18	22.0 ± 2.59	3.4 ± 0.78		
MEA	1.2 ± 0.23	2.3 ± 0.73	2.4 ± 0.61		
Entorhinal	11.3 ± 4.33	24.3 ± 2.73	5.8 ± 1.07		
PTLp	3.4 ± 0.80	1.2 ± 0.76	7.0 ± 1.19	1.3 ± 0.60	4.8 ± 1.68
SSs	1.9 ± 0.71	3.0 ± 0.63	0.3 ± 0.10	1.0 ± 0.38	1.3 ± 0.58
SSp	1.7 ± 1.29	1.3 ± 0.43	1.2 ± 0.33	0.6 ± 0.28	2.8 ± 1.28
Parietal	7.0 ± 2.36	5.6 ± 0.47	8.5 ± 1.40	2.9 ± 1.08	8.8 ± 3.21
VISI	1.2 ± 0.62	0.3 ± 0.17	16.6 ± 1.92	0.6 ± 0.29	6.3 ± 2.60
VISm	2.6 ± 1.45	0.3 ± 0.13	15.8 ± 2.25	1.6 ± 0.91	2.8 ± 1.34
VISp	0.4 ± 0.26	0.0 ± 0.01	7.3 ± 1.66	0.3 ± 0.13	3.4 ± 1.54
Occipital	4.3 ± 2.31	0.6 ± 0.30	39.6 ± 1.99	2.4 ± 1.32	12.4 ± 5.02

<sup>1</sup>The percentage ± standard error of retrogradely labeled cells in each cortical region outside of the target region was calculated for each case and averaged for each target region.

TABLE 3. Density of Retrogradely Labeled Cells in Afferent Regions<sup>1</sup>

Cortical regions	Location of injection sites				
	Area 36	Area 35	POR	LEA	MEA
Piriform	275 ± 83	1318 ± 183	11 ± 4	1062 ± 219	745 ± 412
MOS	133 ± 32	178 ± 38	130 ± 17	54 ± 19	108 ± 69
MOp	27 ± 17	44 ± 13	20 ± 6	12 ± 6	17 ± 6
PL	124 ± 37	152 ± 62	17 ± 6	120 ± 26	32 ± 12
ILA	416 ± 120	326 ± 128	44 ± 22	619 ± 136	171 ± 97
ORBm	512 ± 100	380 ± 118	70 ± 16	728 ± 125	75 ± 42
ORB1	514 ± 174	848 ± 183	23 ± 9	306 ± 92	56 ± 29
ORBvl	460 ± 79	574 ± 179	420 ± 104	561 ± 124	216 ± 135
Frontal	156 ± 35	178 ± 40	76 ± 5	118 ± 16	69 ± 25
Ald	749 ± 174	1036 ± 289	53 ± 13	710 ± 87	102 ± 40
Alv	3238 ± 1765	1918 ± 223	55 ± 22	1454 ± 142	448 ± 251
Alp	1518 ± 262	2808 ± 323	73 ± 25	1650 ± 341	278 ± 111
GU	123 ± 42	262 ± 46	7 ± 4	139 ± 21	30 ± 13
VISC	699 ± 194	1070 ± 269	65 ± 49	238 ± 62	73 ± 28
Insular	649 ± 145	1129 ± 60	44 ± 13	677 ± 62	135 ± 42
AUD	395 ± 187	242 ± 131	423 ± 66	190 ± 107	55 ± 14
AUDv	1549 ± 467	1031 ± 654	362 ± 115	83 ± 30	52 ± 18
Area 35			495 ± 89	2273 ± 270	426 ± 125
Area 36			1361 ± 349	854 ± 134	405 ± 111
TeV	2776 ± 521	818 ± 106	1999 ± 444	200 ± 0	271 ± 0
POR	2547 ± 807	637 ± 396		816 ± 192	798 ± 175
Temporal	2246 ± 254	616 ± 207	1184 ± 182	508 ± 109	304 ± 53
ACAd	61 ± 17	56 ± 23	177 ± 38	88 ± 29	107 ± 56
ACAv	13 ± 7	18 ± 11	71 ± 20	82 ± 54	84 ± 19
RSPd	125 ± 38	29 ± 9	1247 ± 188	107 ± 51	248 ± 97
RSPv	8 ± 4	2 ± 1	280 ± 57	49 ± 41	213 ± 97
Cingulate	76 ± 14	25 ± 10	595 ± 78	85 ± 40	189 ± 64
LEA	1218 ± 295	1739 ± 293	268 ± 55		
MEA	221 ± 31	297 ± 101	350 ± 102		
Entorhinal	567 ± 198	1194 ± 189	299 ± 59		
PTLp	371 ± 113	164 ± 83	2171 ± 845	112 ± 54	290 ± 80
SSs	168 ± 67	311 ± 79	35 ± 10	71 ± 30	48 ± 19
SSp	15 ± 42	95 ± 7	27 ± 7	8 ± 4	24 ± 10
Parietal	138 ± 42	95 ± 7	145 ± 21	30 ± 11	56 ± 18
VISI	109 ± 62	42 ± 25	2840 ± 791	52 ± 26	328 ± 123
VISm	222 ± 189	55 ± 30	2374 ± 324	174 ± 100	169 ± 80
VISp	19 ± 18	5 ± 2	713 ± 149	15 ± 7	108 ± 44
Occipital	147 ± 71	29 ± 15	1696 ± 113	64 ± 34	187 ± 67

<sup>1</sup>The density ± standard error of retrogradely labeled cells per cubic millimeter of cortex was calculated for each case for each of the 29 or 30 afferent regions. Density of retrogradely labeled cells for composite regions, e.g., frontal, was calculated in the same way and thus is not simply an average of the densities of labeled cells in the comprising regions.

these regions are shown in Figure 3. A representative set of cortical borders is shown on camera lucida drawings of coronal sections from one of the experimental brains (Fig. 4).

**Temporal regions.** The perirhinal cortex is comprised of two strips of cortex associated with the most deeply invaginated portion of the rhinal sulcus (Fig. 5A,B). As described here, the perirhinal cortex extends further dorsally than in previous definitions. The region includes the ventral portions of caudal Par2, Te3, and Te2 according to Paxinos and Watson (1986) and the ventral portion of ventral temporal association areas (TeV) according to Swanson (1992). The perirhinal cortex is bordered rostrally by the insular cortex. The insular cortex overlies the claustrum. Thus, the disappearance of the claustrum provides a useful landmark for the rostral border of the perirhinal cortex. Area 35 is a narrow strip of cortex that primarily occupies the ventral bank and fundus of the rhinal sulcus. Area 36 is a broader, more dorsally situated strip that includes much of the dorsal bank of the rhinal sulcus as well as a portion of the dorsally adjacent cortex.

Area 35 is agranular cortex characterized by a broad layer I and by the occurrence of large, darkly staining, heart-shaped pyramidal cells in layer V. Area 36 exhibits a more highly organized cytoarchitecture. It contains a weak granular layer (IV) in which granule cells are intermixed with cells that constitute layers III and V. Layer V is noticeably broader than in area 35 and the cells are smaller and more densely packed. In dorsal portions of area 36, the cortex is organized in a more distinctly

columnar fashion. At caudal levels, area 36 is less radial in appearance and the differences between the dorsal and ventral area 36 are less apparent. Area 36 is distinguished from the dorsally adjacent association cortex by several cytoarchitectonic features (Fig. 5). The association cortex is, in general, more columnar and more distinctly laminated with layer IV clearly more prominent. Layer V is broader and sparsely populated with larger cells. Layer VI is also broader than that of area 36 and is separated from layer V by a cell sparse gap.

The postrhinal cortex (Fig. 5C) includes portions of areas that have previously been described as the perirhinal, entorhinal, and postrhinal cortices (for full discussion, see Burwell et al., 1995). The region includes the most caudal portions of the perirhinal cortex and Te2 and the most ventral portions of Oc2L according to Paxinos and Watson (1986). As compared to Swanson (1992), the postrhinal cortex includes caudal entorhinal cortex and the ventral portion of caudal ventral temporal association cortex. The postrhinal cortex is located caudal to the perirhinal cortex and dorsal to the rhinal sulcus. It has a bilaminar appearance; layers II and III are continuous and fairly homogeneous and the cells of layers V and VI exhibit similar staining characteristics. It does, however, have a weak granular layer. The postrhinal cortex can be distinguished from the dorsally adjacent association cortex primarily on the basis of its comparatively weaker layer IV. The postrhinal cortex is bordered medially by the cytoarchitectonically distinct agranular retrosplenial cor-

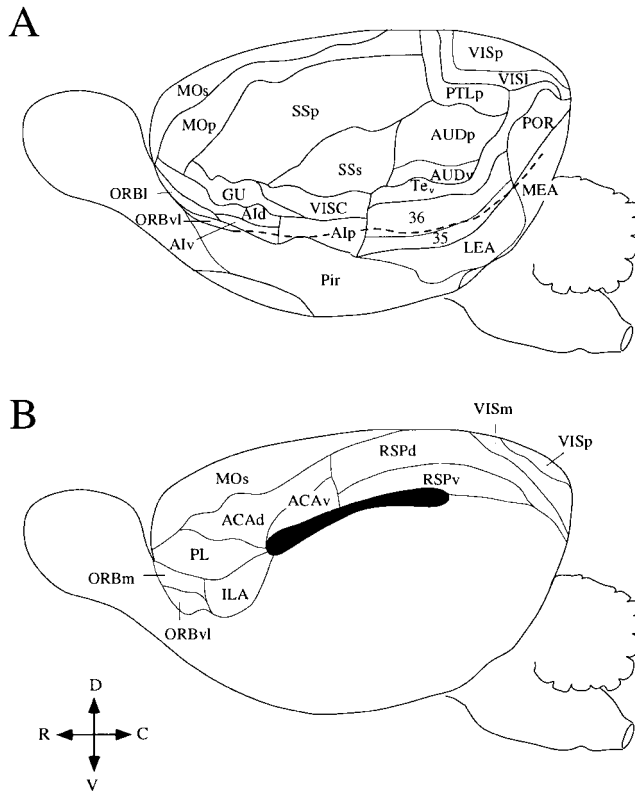


Fig. 3. Cortical boundaries for all cortical regions quantified are shown on lateral (A) and medial (B) surface views of the rat brain. ACAd, dorsal anterior cingulate area; ACAv, ventral anterior cingulate area; AId, dorsal agranular insular area; AIv, ventral agranular insular area; Alp, posterior agranular insular area; AUD, primary auditory area; AUDp, posterior auditory area; AUDv, ventral auditory area; c, caudal; d, dorsal; GU, gustatory area; LEA, lateral entorhinal area; MEA, medial entorhinal area; MOs, secondary motor areas; MOp, primary motor area; ORBl, lateral orbital area; ORBm, medial orbital area; ORBvl, ventrolateral orbital area; Pir, piriform cortex; PL, prelimbic area; POR, postrhinal cortex; PTLp, posterior parietal association areas; r, rostral; RSPd, dorsal retrosplenial area; RSPv, ventral retrosplenial area; SSs, primary somatosensory area; SSs, supplementary somatosensory area; Te<sub>v</sub>, ventral temporal association areas; v, ventral; VISC, visceral area; VISl, lateral visual areas; VISm, medial visual areas; VISp, primary visual area; 35, area 35 of the perirhinal cortex; 36, area 36 of the perirhinal cortex.

tex (Vogt, 1985) and ventrally primarily by the entorhinal cortex. In the caudomedial portion, however, its ventral border is with a thin band of the parasubiculum that is interposed between the entorhinal and postrhinal cortices.

Despite the expanded fields designated as the perirhinal and postrhinal cortices, a dorsally adjacent strip of cortex remains that corresponds to the dorsal aspect of Swanson's (1992) Te<sub>v</sub>. This narrow strip of cortex is both cytoarchitectonically and connectionally distinct from area 36, from the postrhinal cortex, and from regions dorsally adjacent. Te<sub>v</sub> is characterized by a regular, compressed layer II, a recognizable layer IV, and cell-sparse gaps above and below layer V. Layer III contains small pyramidal cells and layer V contains large darkly staining pyramidal cells. Rostrally, area 36 is most easily distinguished from Te<sub>v</sub> by differences in layer V. The pyramidal cells in layer V of the dorsal portion of area 36 are smaller and not as darkly stained as in Te<sub>v</sub>. These features are less distinct at more caudal levels. Caudal area 36 and the postrhinal cortex

can be most easily distinguished from Te<sub>v</sub> by the latter's cell-sparse bands located deep and superficial to layer V. Te<sub>v</sub> can be distinguished from the dorsally adjacent cortex, especially from visual regions, because it has a less prominent layer IV. It is also distinguished from auditory cortex by its layer V which is narrower and more densely populated than layer V of the auditory areas.

**Entorhinal cortex.** The nomenclature used for the entorhinal cortex is based on classical descriptions of this region (Blackstad, 1956; Brodmann, 1909; Kreig, 1946a). The entorhinal cortex is subdivided into a lateral entorhinal area and a medial entorhinal area (Fig. 1). The LEA is roughly triangular-shaped and is bordered dorsally by the perirhinal and postrhinal cortices and rostrally by the piriform and periamygdaloid cortices (Fig. 1B). The LEA is bordered caudally and medially by the MEA. The MEA, which encompasses a substantial portion of the caudal pole of the cortical mantle, is bordered medially by the parasubiculum (Dolorfo and Amaral, 1998). The LEA (Fig. 5B) is distinguished from the laterally adjacent area 35 and postrhinal cortices by the large darkly staining cells in layer II and the presence of a thin lamina dissecans (cell-sparse layer between layers III and V). The MEA (Fig. 5C) can be distinguished from the LEA by characteristics of layers II and III. Layer II of MEA contains lighter staining neurons that produce a slightly thicker and more continuous layer. The neurons in the superficial portion of layer III are more densely packed in MEA than in LEA. Layers II and III are separated by an acellular space and the lamina dissecans is more prominent than in the LEA.

**Frontal regions.** A total of seven frontal regions were examined. These include the primary and supplementary motor areas (MOp and MOs), prelimbic area (PL) and infralimbic areas (ILA), and the medial, lateral, ventral, and ventrolateral orbital areas (ORBm, ORBl, ORBv, and ORBvl, respectively). Cytoarchitectonic features used for borders for MOp and MOs are as described by Donoghue and Wise (1982). Microstimulation studies, as well as cytoarchitectonic and connectional criteria, clearly define MOp as a motor area similar to MI in the monkey (Donoghue and Wise, 1982). The description of MOs as a supplementary motor area is based on similarities to MII in the monkey, i.e., it has corticospinal connections and receives input from the mediodorsal nucleus of the thalamus (Beckstead, 1976; Krettek and Price, 1977). The criteria and nomenclature for the remaining five regions are from Krettek and Price and are based primarily on connections with the mediodorsal nucleus of the thalamus (1977).

**Insular regions.** The insular cortex was divided into dorsal, ventral, and posterior agranular insular areas (AId, AIv, and Alp, respectively). We have followed the borders and nomenclature of Krettek and Price (1977) for these regions. There were also two granular regions: the gustatory area (GU) and the visceral area (VISC). Nomenclature is from Swanson (1992).

**Cingulate regions.** Cingulate regions include the dorsal and ventral anterior cingulate areas (ACAd and ACAv) that were defined according to Krettek and Price (1977; but see also Vogt and Peters, 1981). Also included are the agranular retrosplenial area (Fig. 3, RSPd) and the granular retrosplenial area (RSPv; Krettek and Price, 1977; Vogt and Miller, 1983).

**Parietal regions.** Cytoarchitectonic features used for distinguishing primary and supplementary somatosen-

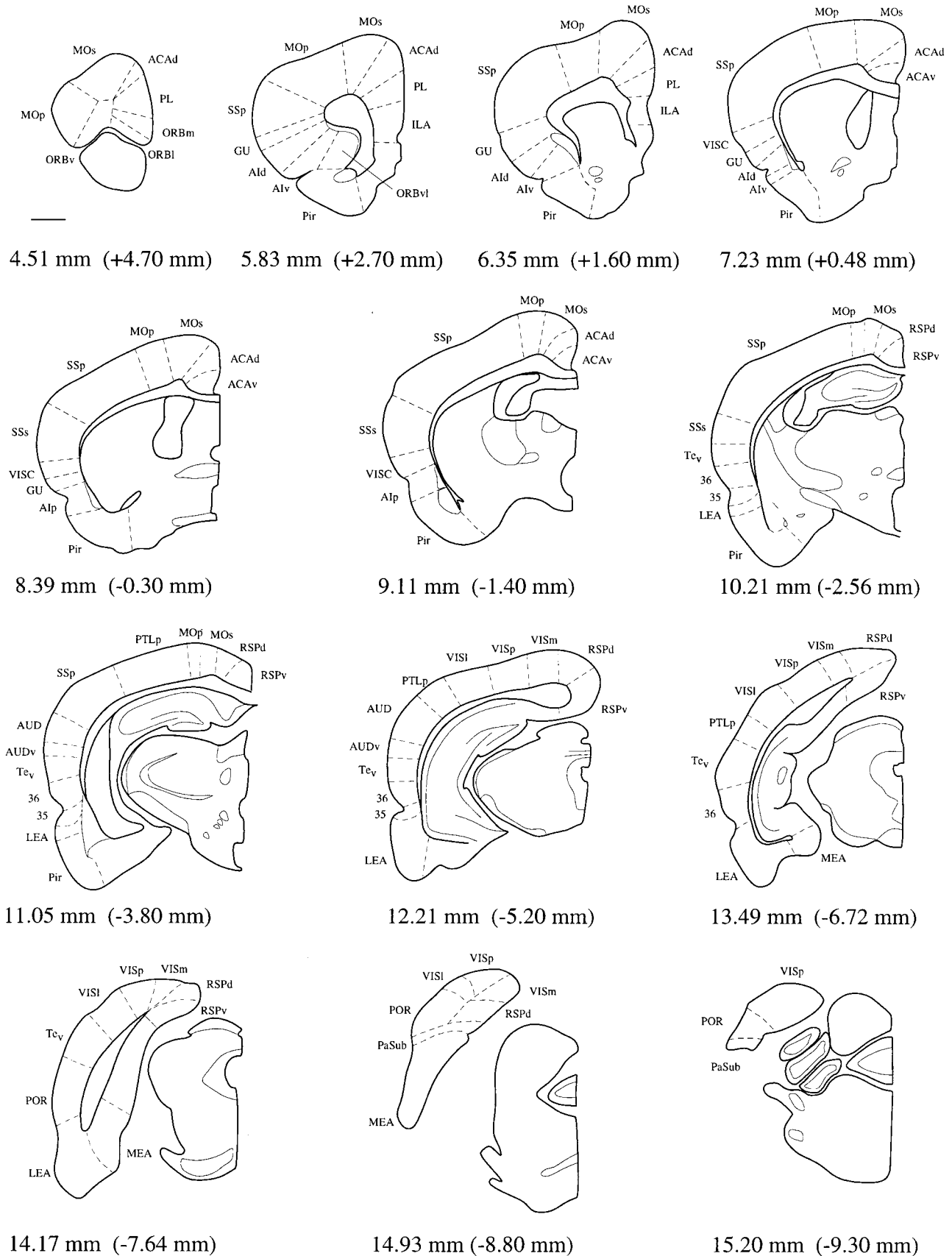


Fig. 4. Cortical boundaries for all cortical regions quantified for a subset of coronal sections of a representative experimental brain. For abbreviations, see list. Scale bar = 1 mm.

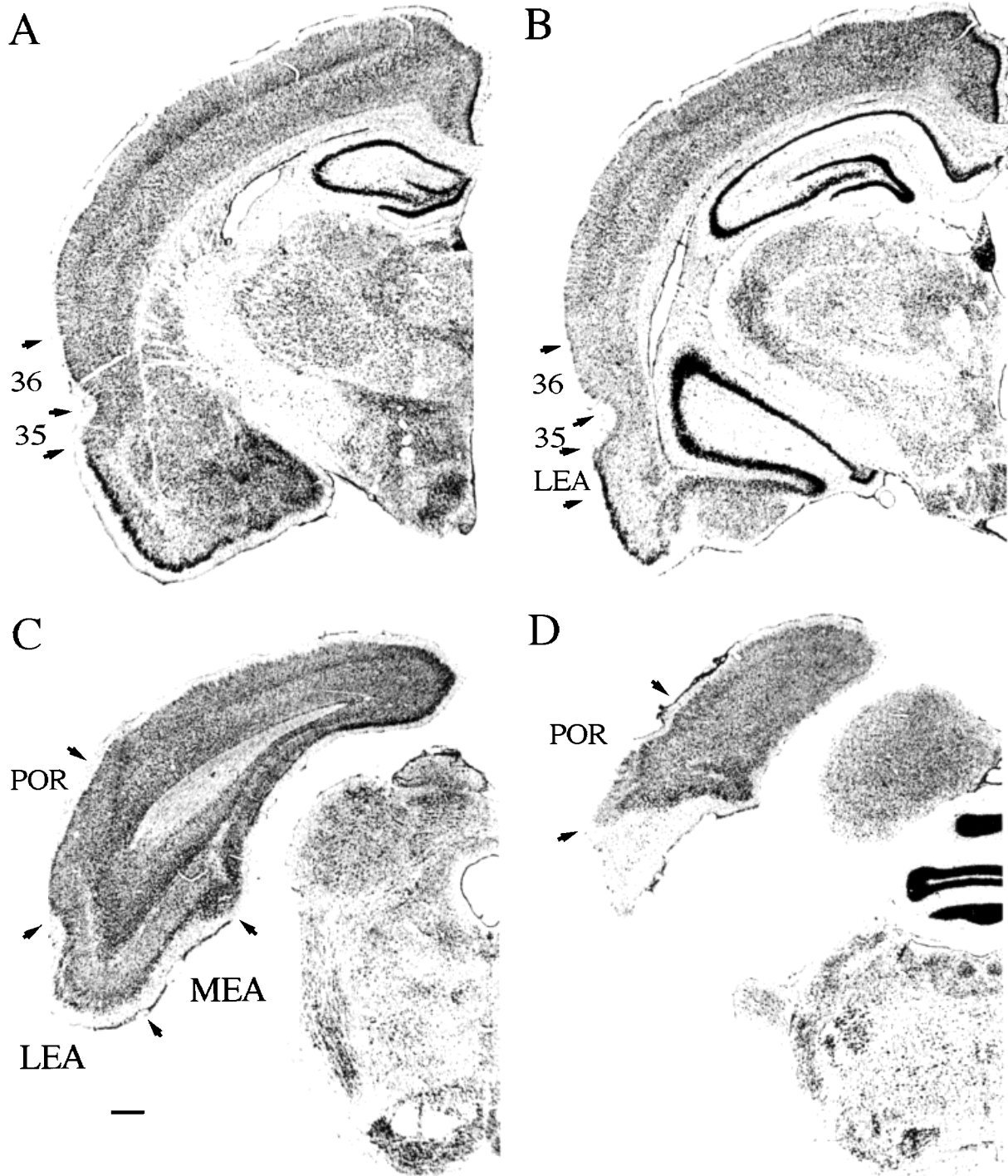


Fig. 5. Nissl-stained sections showing cortical boundaries of the target regions, area 36 (36) and area 35 (35) of the perirhinal cortex, the postrhinal cortex (POR), and the lateral and medial entorhinal areas (LEA and MEA) of the entorhinal cortex. Arrows indicate cytoarchitectonic boundaries. Each panel was digitally scanned into

Adobe Photoshop at 600 dpi using a Wild MZ-6 stereomicroscope (Leica, Inc., Deerfield, IL) coupled to a Leaf Lumina scanning camera (Leaf Systems, Inc., Southborough, MA). The images were then adjusted for brightness and contrast. For abbreviations, see list. Scale bar = 500  $\mu$ m.

sory areas (SSp and SSs) were adopted from Chapin and Lin (1984; see also Sanderson et al., 1984). A posterior parietal region was first identified by Krieg (1946a) and here called PTLp (Swanson, 1992). This is a long strip of

cortex that extends laterally from near the midline at rostral levels and then turns caudally, forming an "L" shape. This can be seen in the surface view in Figure 3. Thus, the posterior parietal cortex can be thought of as

having a rostradorsal limb and a caudal limb. The region receives input from the lateral posterior nucleus of the thalamus and may be homologous to the posterior parietal region in primates (Chandler et al., 1992; Hughes, 1977; Miller and Vogt, 1984). This cortex is characterized by a weak, thin layer IV; overall this cortex is thinner than adjacent cortical areas.

**Unimodal sensory regions.** The definition of auditory cortex was based on the criteria of Arnault and Roger (1990), but corresponds roughly to the descriptions of Swanson (1992) and Paxinos and Watson (1997). Swanson (1992) identified three regions, the primary auditory region (AUD) and dorsal and ventral associational regions. We were unable to reliably identify the border between the primary auditory cortex and the dorsal belt region. Thus, we combined Swanson's dorsal auditory cortical region with the primary auditory region and called it AUD. A ventral supplementary region (AUDv) was also identified.

For the demarcation of the primary visual area (VISp), we followed Swanson (1992). For the visual associational areas, we followed Paxinos and Watson (1997) and defined one lateral and one medial region (VISl and VISm, respectively).

The piriform area was the sole olfactory region examined. The nomenclature and boundaries for this region are well established (Haberly and Price, 1978; Kreig, 1946b; Rose, 1929).

### Description of injection sites

Thirty-seven injections were selected from a library of 72 retrograde tracer injection sites in and around the perirhinal, postrhinal, and entorhinal cortices. Figure 6 shows the locations of the retrograde tracer injection sites that were chosen for quantitative analysis. Because multiple tracers were injected in some experimental cases, the injection sites are indicated by the number of the case and a suffix denoting the type of tracer. The effective injection site was defined as the dye core plus the region of heavy necrosis immediately surrounding the dye core (Fig. 7A). The approximate size and the laminar location of the injection sites in each region are summarized in Table 1. Figure 7 shows retrogradely labeled cells from a representative case in the perirhinal (Fig. 7B) and entorhinal (Fig. 7B,C) cortices. Figures 8 through 12 show computer-generated plots of the locations of labeled cells in a sample of coronal sections for representative injections located in areas 36, 35, the postrhinal cortex, LEA and MEA.

For the afferent regions examined in each experiment, both the percentage of input to the target region and the density of labeling in the afferent regions are presented (Tables 2 and 3). We report both measures for the following reasons. The percentage of total input from an afferent region provides an indication of its relative "influence" on the target region, i.e., of all the cells that project to region X, 30% are located in region Y. If region X receives 10% input from 7 other areas, then a rough summary statement is that region Y has more influence on X than the other areas. This conclusion can be biased by the size of the various afferent regions; if an afferent source is three times as large as another it will be more likely to contribute more projections. The conclusion is also hampered by the lack of knowledge concerning the number and types of synapses that each afferent region makes in the recipient region. The density of labeled cells, by comparison, provides a measure that is corrected for volume. By this measure we

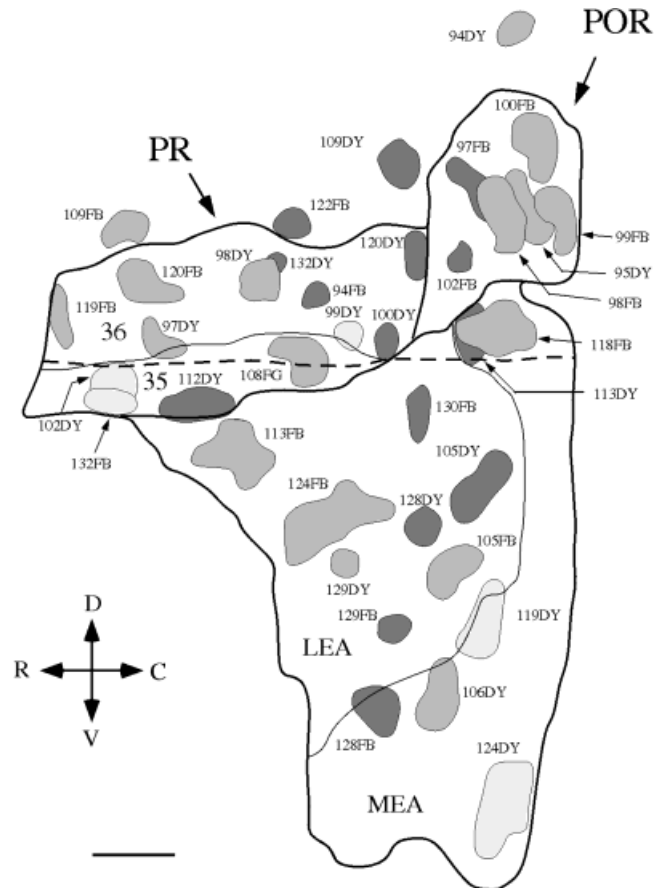


Fig. 6. Representative unfolded map of the perirhinal (PR, areas 35 and 36), postrhinal (POR), and entorhinal (EC, areas LEA and MEA) cortices showing the location of the 37 retrograde injection sites selected for analysis. Sites shown in dark gray are restricted to deep layers. Sites shown in light gray are restricted to superficial layers. Sites shown in middle gray involve both deep and superficial layers. c, caudal; d, dorsal; DY, Diamidino yellow; FB, Fast blue; FG, Fluoro-Gold; r, rostral; v, ventral. Arrows indicate cytoarchitectonic boundaries. Scale bar = 1 mm.

are describing how many retrogradely labeled cells per unit area are located in a region. Initial observations of the data suggested that the two measures might not provide the same information for a number of afferent regions. This was confirmed by a statistical analysis. For each retrograde tracer experiment, the percentage of input from a particular afferent region was significantly correlated with the density of retrogradely labeled cells in that region ( $r \geq .30$ ,  $P < .05$ ). However, for 22 of 34 regions,  $r^2$  was less than 0.50, indicating that more than half of the information provided by the measure "proportion of retrogradely labeled cells" was not duplicated by the measure "density of labeling." Thus, we decided to report both measures of connectivity. In general, we have used percentages to describe the complement of cortical afferents to a single region and density to make comparisons across regions. In all cases, we attempted to emphasize the measure that seemed most appropriate to the question being addressed. Whenever the two measures differed, both were discussed in the results.

As shown in Table 1, there was variation in the size of injection sites. However, there were no significant differ-

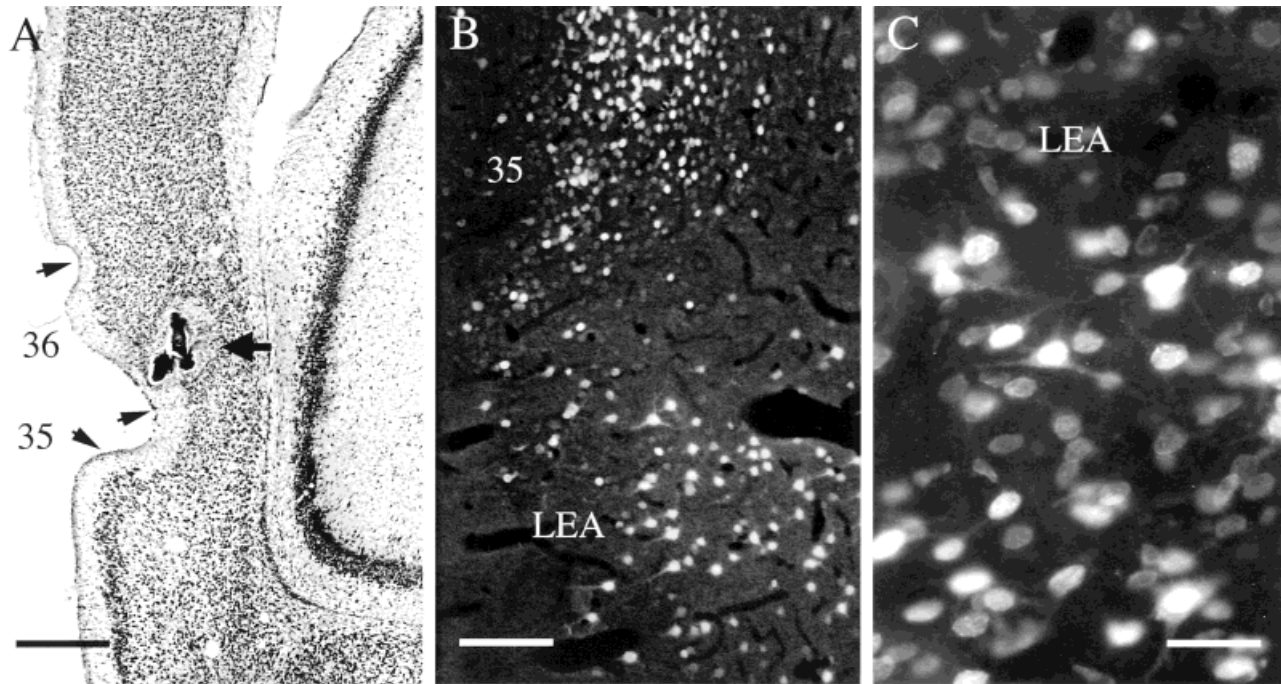


Fig. 7. Neuroanatomical material from a representative case, PR098. Each photomicrograph was taken using a Nikon Optiphot-2. Film was developed and scanned into Adobe Photoshop at 2700 dpi using a Nikon Coolscan film scanner. The images were then enlarged and adjusted for brightness and contrast. **A:** Coronal section stained for Nissl showing the location of a Diamidino Yellow injection site. The

Fast Blue injection site was located in the postrhinal cortex of this case. **B:** Retrogradely labeled cells in the perirhinal and entorhinal cortices. **C:** Retrogradely labeled cells in the entorhinal cortex at higher magnification. Double-labeled cells were clearly identifiable. 35, 36, areas 35 and 36; LEA, lateral entorhinal area. Scale bars = 500  $\mu\text{m}$  in A, 200  $\mu\text{m}$  B, 100  $\mu\text{m}$  C.

ences among the five target regions in mean volume of the injection sites ( $P > .62$ ). Moreover, within a region, the patterns of input were often highly correlated across injection sites even when the volume of the injection site was substantially different. For example, in the LEA the distribution of retrograde labeling for experiments 124FB and 129DY were highly correlated ( $r = 0.94$ ), but the injection sites were 0.32 and 0.05 cu mm, respectively. Because there is no reason to think that there were any regional differences in the efficacy of transport or labeling, it is appropriate to make comparisons across target regions based on the densities of retrogradely labeled cells.

The variability of the percentages and densities of retrograde labeling resulting from different injection sites within a target region might also be of interest. As shown in Tables 2 and 3, the standard errors are fairly small for both percentages and densities of input from afferent areas for each of the target regions. Moreover, correlation analyses confirmed that the profile of cortical input was generally quite similar across injection sites within a particular target region, i.e., percentages of input for injection sites placed closely together tended to be highly correlated. For injection sites located in area 35, the strength of correlations across percentages of input from the different afferent regions ranged from  $r = 0.88$  to  $r = 0.95$ . Similar analyses for postrhinal cortex (POR) indicated that the intercorrelations ranged from  $r = 0.47$  to  $r = 0.94$ , although the majority of  $r$  values were above 0.76. For the LEA, correlations ranged from  $r = 0.60$  to  $r = 0.97$ . There was more regional variation in the MEA. The three injections located in the more rostral and medial portions

(119DY, 106DY, and 128DY) were intercorrelated at  $r = 0.87$  or higher. The three injections located in the caudal portions (113DY, 118DY, and 124DY) were intercorrelated at  $r = 0.54$  or higher. These two sets of injection sites were not significantly correlated with each other (values ranged from  $r = -0.13$  to  $r = 0.18$ ). The highest regional variation for percentages of input was found for area 36; however, even for that region, injection sites located near to one another tended to be highly correlated. For example, percentages of input to 99DY and 100DY in caudal area 36 were significantly correlated ( $r = 0.47$ ), but neither was significantly correlated with percentages of input to 120FB in rostral area 36 ( $r = -0.09$  and  $r = 0.04$ , respectively). The patterns of intercorrelations within target regions were similar for the density measures.

### Afferents to the perirhinal cortex

**Piriform area.** Area 36 receives an average of 5.6% of its total cortical input from the piriform cortex. The projections originate from caudal portions of the piriform cortex (primarily from layer III) and terminate in the superficial layers. Area 35 receives an average of 25.6% of its cortical input from the piriform cortex (see Fig. 9A–E). In contrast to area 36, rostral levels of the piriform cortex provide the heavier input to area 35. The projection arises primarily from layer III of all rostrocaudal levels of piriform cortex, but rostral area 35 also receives input from layer II. The projection to area 35 terminates preferentially in superficial layers. The piriform cortex projects

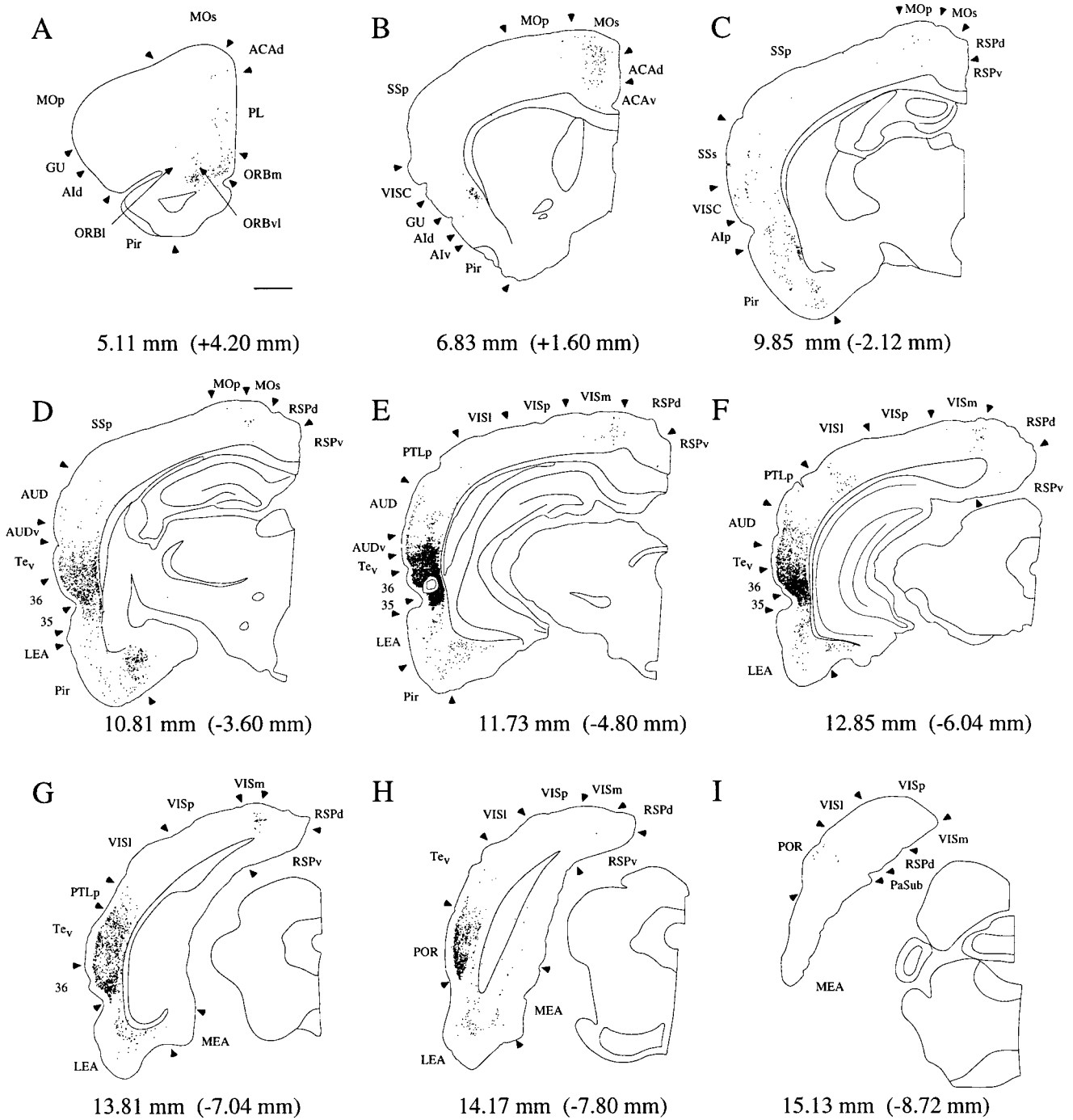


Fig. 8. A-I: Computer-generated plots of coronal sections showing the location of a retrograde tracer injection in area 36 of the perirhinal cortex and the distribution of retrogradely labeled cells arising from

that injection site. Nine of 43 rostrocaudal levels are shown for experiment 98DY. Arrows indicate cytoarchitectonic boundaries. For abbreviations, see list. Scale bar = 1 mm.

more heavily to rostral area 35. Thus, rostral portions of area 35 receive 30–35%, whereas caudal regions receive 15–20%, of their input from piriform cortex.

**Frontal areas.** Areas 36 and 35 receive similar amounts (8%) and patterns of input from frontal cortical areas. Moreover, the composition of input from different frontal regions is roughly the same. About half of the

frontal input is from motor regions, primarily MOs (Fig. 9B). Another 3% arises in orbital frontal regions (ORBm, ORBl, ORBvl), and the remaining 1% from medial frontal regions (PL and ILA). Examination of data from individual experiments revealed that the origins of frontal-perirhinal projections terminate throughout areas 35 and 36. The projections originate primarily in layers II/III.

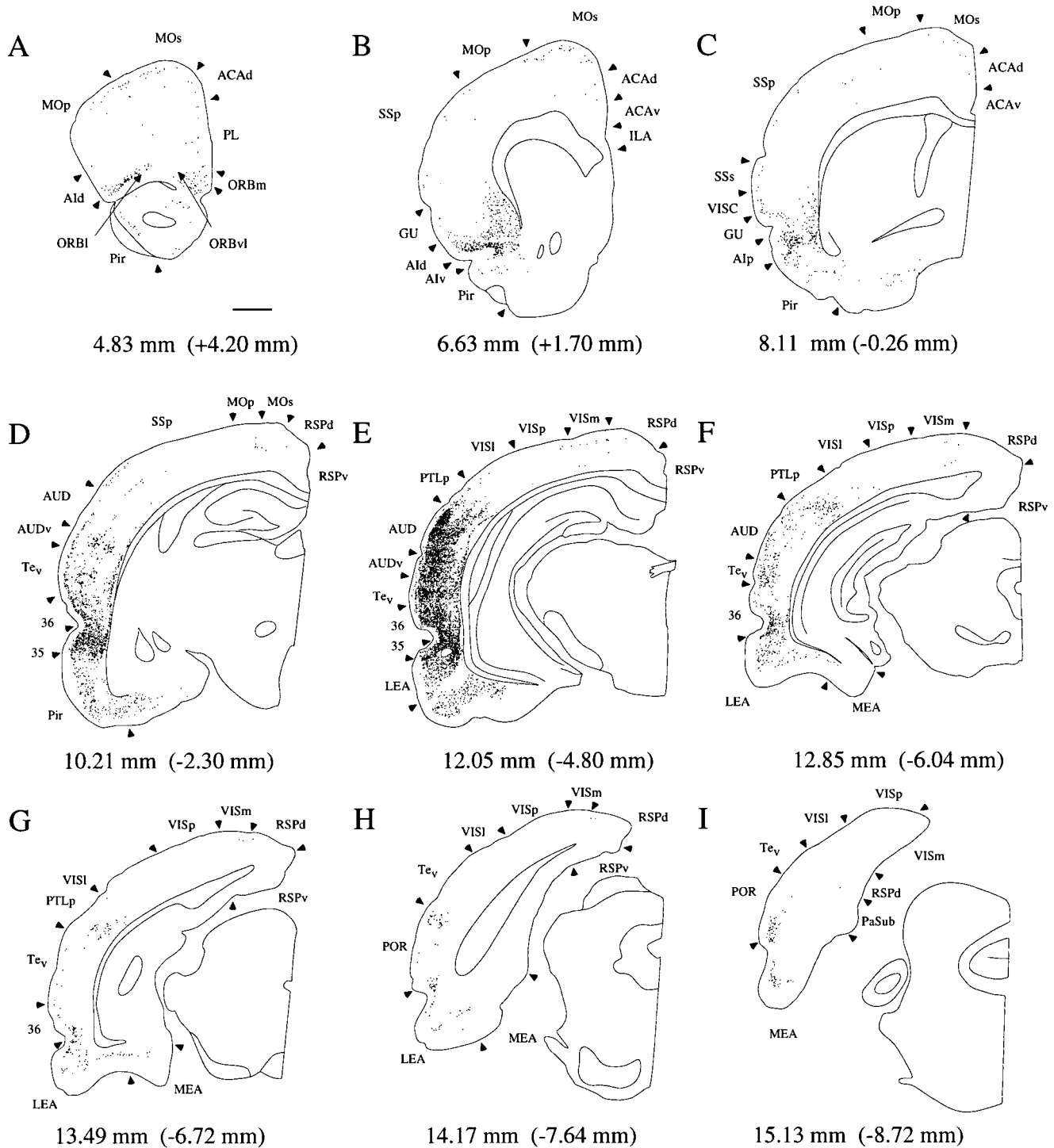


Fig. 9. A-I: Computer-generated plots of coronal sections showing the location of a retrograde tracer injection in area 35 of the perirhinal cortex and the distribution of retrogradely labeled cells arising from

that injection site. Nine of 44 rostrocaudal levels are shown for experiment 112DY. Arrows indicate cytoarchitectonic boundaries. For abbreviations, see list. Scale bar = 1 mm.

Examination of the density data produced a slightly different picture. The density of retrogradely labeled cells was substantially greater in the orbitofrontal regions and in ILA than in supplementary motor cortex.

**Insular areas.** Area 36 receives almost 13% of its total input from insular regions, primarily from agranular

insular cortex (9.9%). The largest portion arises from the Alv, somewhat less from the other agranular areas (Ald and Alp). Granular insular areas provide little input to area 36 and that arises mostly from caudal VISC. The origins of both the agranular and granular insular input are in layer II and possibly superficial layer III. Ventral

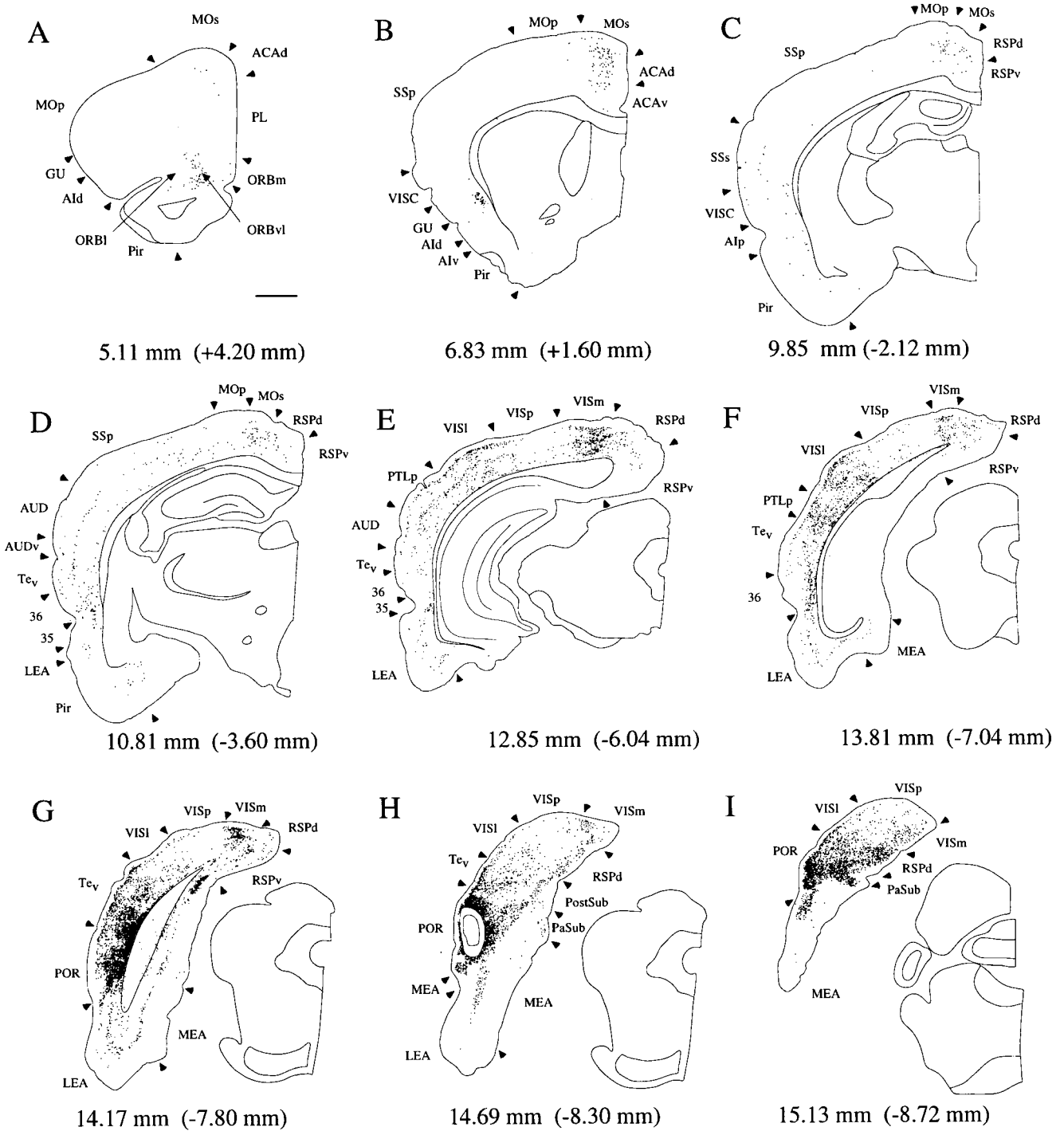


Fig. 10. A-I: Computer-generated plots of coronal sections showing the location of a retrograde tracer injection in the postrhinal cortex and the distribution of retrogradely labeled cells arising from that

injection site. Nine of 43 rostrocaudal levels are shown for experiment 98FB. Arrows indicate cytoarchitectonic boundaries. For abbreviations, see list. Scale bar = 1 mm.

portions of area 36 receive a greater proportion of insular input than dorsal portions.

The insular cortex provides roughly 22% of the total input to area 35. Observation of the individual experiments revealed that the patterns of insular input are quite similar to all levels of area 35 (for example, see Fig. 9B,C).

As with area 36, a large proportion of the input arises in agranular insular cortex and less arises in granular areas, particularly GU. Also similar to area 36, the projections originate primarily in layer II. A final similarity is that only the caudal portion of VISC provides input to area 35.

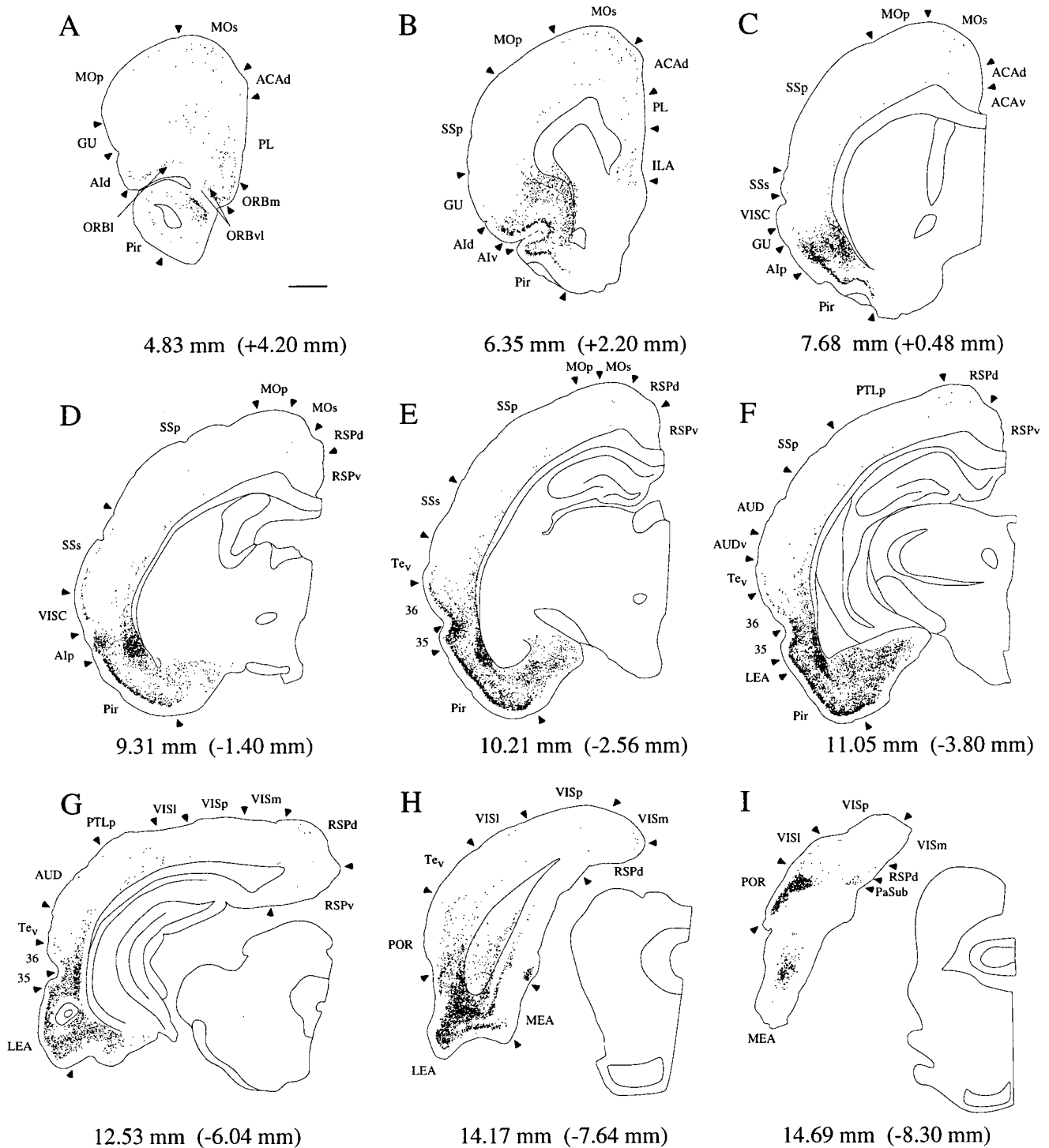


Fig. 11. A-I: Computer-generated plots of coronal sections showing the location of a retrograde tracer injection in the lateral entorhinal area (LEA) of the entorhinal cortex and the distribution of retrogradely labeled cells arising from that injection site. Nine of 48

rostrocaudal levels are shown for experiment 124FB. Arrows indicate cytoarchitectonic boundaries. For abbreviations, see list. Scale bar = 1 mm.

**Temporal areas.** Perirhinal areas 35 and 36 differ dramatically in the amount of input they receive from temporal areas. This difference is apparent in both the percentages of input and in the density of labeled cells in

the temporal regions. Temporal regions provide the major cortical input to area 36 (49.7%). The greatest proportion, 30.4%, originates in area Te, and terminates in all portions of area 36. The postrhinal cortex and the auditory regions

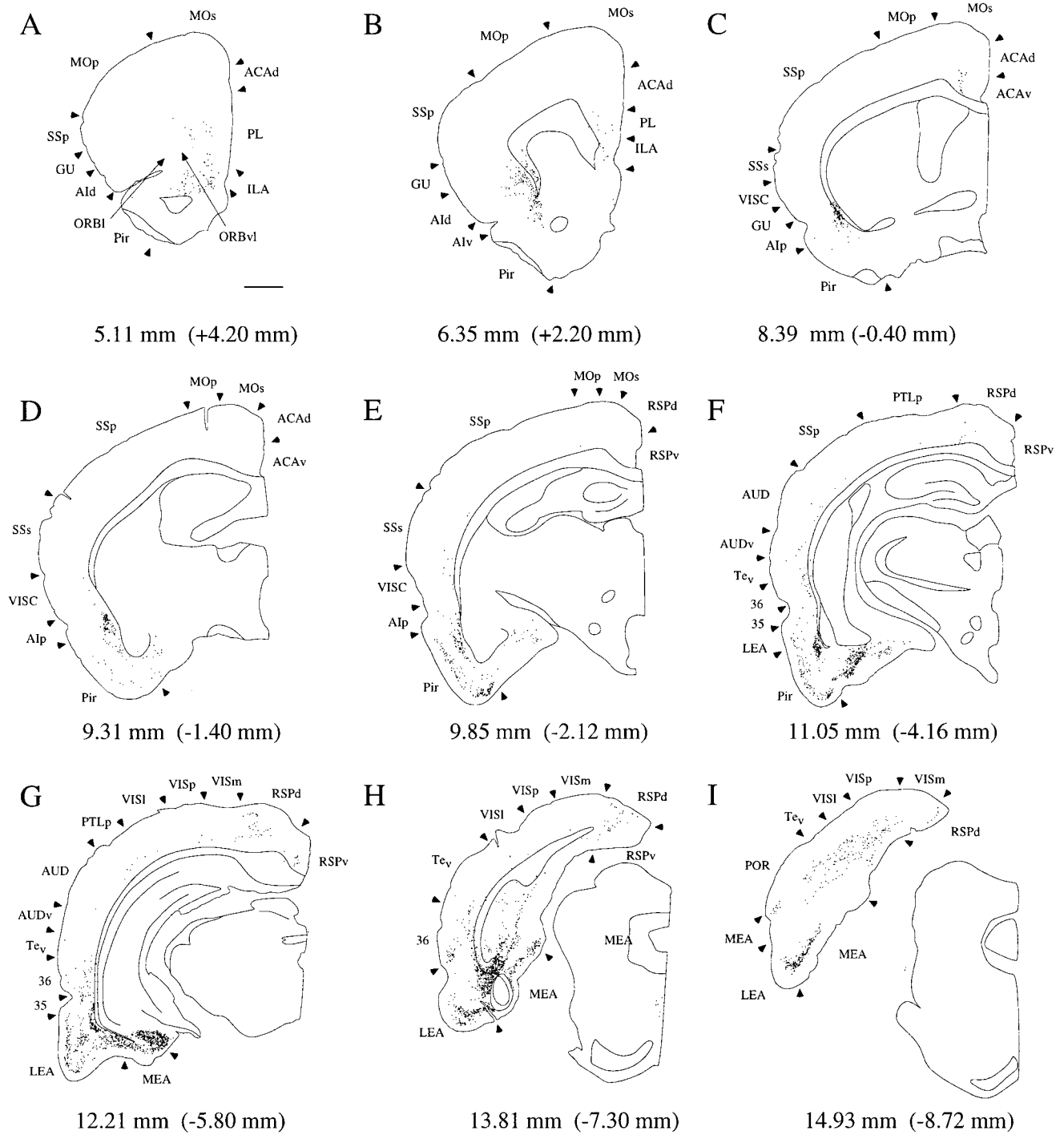


Fig. 12. **A-I**: Computer-generated plots of coronal sections showing the location of a retrograde tracer injection in the MEA of the entorhinal cortex and the distribution of retrogradely labeled cells

arising from that injection site. Nine of 44 rostrocaudal levels are shown for experiment 106DY. Arrows indicate cytoarchitectonic boundaries. For abbreviations, see list. Scale bar = 1 mm.

also provide substantial proportions (10.5% and 8.7%, respectively) of the total input to area 36. The POR projection originates in the rostral portion of the region and preferentially innervates caudal area 36 (Fig. 8H). The auditory regions, in contrast, preferentially innervate rostral area 36.

In contrast to area 36, area 35 receives relatively little input from temporal regions (12.7%). The largest proportion of this input comes from Te<sub>v</sub>, and terminates preferentially at caudal levels of area 35. The next largest input arises in auditory areas. Although the percentage of input

is small, the density of retrogradely labeled cells in auditory association cortex was greater than in  $Te_v$ .

The temporal cortical projections to perirhinal areas 35 and 36 originate primarily in layers II/III in POR and in layers II, V, and deep VI of other temporal regions.

**Cingulate areas.** Area 36 receives relatively little input from the cingulate cortex and area 35 receives even less. These meager cingulate projections arise from the dorsal subdivisions of the anterior cingulate cortex and from the retrosplenial cortex. Scattered, retrogradely labeled cells were observed in layers II/III and V. The retrosplenial input originates primarily from caudal portions of RSPd. Otherwise, there is no apparent topography to the cingulate-perirhinal projections.

**Entorhinal areas.** As described in more detail in a previous study (Burwell and Amaral, 1998), the entorhinal projection to the perirhinal cortex arises almost exclusively from the LEA, and the projections are much stronger to area 35 than to area 36 (22% as compared to 10.1%). The projection from the MEA accounts for only 1% or 2% of the perirhinal cortex input. In general, the perirhinal projections originate in layers III and V.

**Parietal areas.** Area 36 receives an average of 7.0% of its input from parietal areas. The parietal projections to area 36 originate from caudal levels of the parietal cortex. The origin of the input is distributed across SSs, SSp, and PTLp, but the largest proportion arises in PTLp. PTLp and SSs project more heavily to rostral area 36 than to caudal area 36. Only the rostral extreme of area 36 receives any input from the primary somatosensory area (SSp, Fig. 8, experiment 119FB).

In contrast to area 36, all rostrocaudal levels of area 35 receive about 5% of their input from parietal cortices; the largest portion arises in SSs. Rostral parietal cortex projects rostrally in area 35 and caudal levels project caudally. In all cases, the projections arise in layers II, superficial V, and deep VI.

**Occipital areas.** About 4% of the input to area 36 originates from visual association cortices (VISl and VISm) and this terminates in the extreme caudal perirhinal cortex. The projections originate at all rostrocaudal levels but are strongest from caudal levels of VISm. Layers II, V, and VI give rise to the projections. Little or no input from visual cortex reaches the remaining portions of area 36 or any portion of area 35.

### Afferents to the postrhinal cortex

**Piriform areas.** The postrhinal cortex receives little or no input from piriform cortex. The only retrogradely labeled cells that were observed were near the borders with either orbital or insular cortex.

**Frontal areas.** Less than 4% of the total cortical input to the postrhinal cortex originates in the frontal cortex. MOs provides the majority of that input. The MOs projection arises near the border with ACAd, primarily in layer V, but also from layers II and VI. ORBvl provides the next largest input, primarily arising in layer II. Although this projection provides less than 1% of the total frontal input to the postrhinal cortex, the density of retrogradely labeled cells was higher than in MOs, which is a substantially larger region. The ORBvl projection is heavier to the caudal portions of postrhinal cortex.

**Insular areas.** The postrhinal cortex receives very little input from insular cortex. The meager input arises in

deep and superficial layers and terminates primarily in rostroventral postrhinal cortex.

**Temporal areas.** Almost 28% of the total input to postrhinal cortex originates in temporal cortical areas. The largest proportion of the input arises in area  $Te_v$ , followed by area 36. These projections arise from all rostrocaudal levels of  $Te_v$  and area 36, primarily in layers II, VI, and to a lesser extent, V. The terminations exhibit no obvious areal or laminar topography. Interestingly, a smaller projection appears to arise in the auditory region, AUD. Labeled cells were observed almost exclusively in the extreme posterior portion of this region in a belt of auditory association cortex that surrounds primary auditory cortex (Arnault and Roger, 1990). The auditory projections terminate in all portions of the postrhinal cortex, but are slightly stronger to ventral and caudal portions.

**Cingulate areas.** Of the cingulate areas, the retrosplenial cortex provides the strongest input (over 12%) to the postrhinal cortex, with the largest amount arising in RSPd. All portions of RSPd project to all portions of the postrhinal cortex. The projections arise primarily in layer V, but a few retrogradely labeled cells were also observed in layer II. RSPv also projects to the postrhinal cortex, but less strongly. The topography and laminar pattern of this projection are similar to that described for RSPd with the exception that only the portion of RSPv near the border with RSPd gives rise to the projection.

The caudal portion of dorsal anterior cingulate cortex provides a meager input to the postrhinal cortex that arises primarily in layer V and terminates more heavily in caudal portions of the postrhinal cortex. ACAv provides little or no input to the region.

**Entorhinal areas.** The entorhinal projection to the postrhinal cortex arises in both LEA and MEA. The total entorhinal input, averaged over all portions of the postrhinal cortex, is less than 6%. Dorsal postrhinal cortex receives only a meager projection, whereas ventral portions receive approximately 8% of their total input from entorhinal areas. The percentage of input arising from the MEA is less than that arising from the LEA. The density of labeled cells, however, is higher in the MEA than in the LEA. Rostral postrhinal cortex receives more of its entorhinal input from the LEA, and caudal postrhinal cortex receives more input from the MEA. The entorhinal projections arise in deep and superficial layers.

**Parietal areas.** The parietal input to the postrhinal cortex arises primarily from posterior parietal cortex (PTLp, Fig. 10E,F) and accounts for 7% of the region's total input. Layer V provides the predominant input with somewhat less arising in layers II and VI. All portions of the posterior parietal cortex project to the postrhinal cortex, but the rostradorsal limb projects more heavily to rostral POR and the caudal limb projects more heavily to caudal POR. Interestingly, a small input appears to arise from primary somatosensory cortex (SSp), but the input arises entirely from the portion of SSp that lies adjacent to the rostral border of the dorsal limb of PTLp. This region may be a transitional area between SSp and PTLp. The overall weakness of the SSp input is apparent in the density data (Table 3). The density of labeled cells in either somatosensory area was less than 30 cells per cu mm. The density of labeled cells in PTLp, by contrast, was 1,698 cells per cu mm or more than 70 times that of the somatosensory cortex.

**Occipital areas.** Input from the visual association cortices (VISl and VISm) accounts for approximately one-third of the total input to the postrhinal cortex. Layers II, V, and VI give rise to the projections, but generally more labeled cells were observed in layer V. All rostrocaudal portions of visual association cortex project to all portions of the postrhinal cortex. The input from posterior medial areas, however, is slightly weaker to the rostral POR. Some input also arises in primary visual cortex (VISp, see Fig. 10E–G for an illustration of the relative densities of labeling in visual associational cortices and primary visual cortex). The input from VISp tended to originate in layer VI and sometimes layer II. In some cases, dense bands of retrogradely labeled cells were observed in layers II and V near VISm. This suggests either that the border between VISp and VISm was misplaced in some cases or that there is a transitional area interposed between the two regions. In either case, the estimates of input from VISp to POR may be slightly inflated.

### Afferents to the entorhinal cortex

**Piriform areas.** Both subdivisions of the entorhinal cortex receive roughly one-third of their cortical input from the piriform cortex. The density of retrograde cell labeling in the piriform cortex following LEA injections was substantially heavier than that following MEA injections (see Figs. 11 and 12 for representative examples). The projections arise in layer II of the piriform cortex at all rostrocaudal levels.

Whereas the average amount of piriform input to the LEA and MEA is similar, there are some rather striking subregional differences in the patterns of the terminations. Rostrolateral LEA receives roughly 45% of its input from the piriform cortex, whereas caudomedial LEA receives only about 16%. Within the MEA, the portion situated near its rostralateral border with the LEA receives 60% of its total input from the piriform cortex (Fig. 6, injection sites 119DY, 106DY, and 128FB). Locations nearer the parasubiculum, in the extreme caudolateral and caudomedial MEA, receive on average less than 2% of their input from the piriform cortex and this figure is largely accounted for by labeling resulting from a single injection site (Fig. 6, injection sites 113DY [0.1%], 118FB [5%], and 124DY [0.5%]).

**Frontal areas.** The two subdivisions of the entorhinal cortex receive roughly equal proportions of their input from frontal regions (about 10%), but there are differences in the composition of that input. The origin of the input to LEA is fairly evenly distributed across all frontal areas, whereas the largest proportion of the input to MEA arises in MOs. Interestingly, the MOs input to the MEA terminates exclusively in the portion that borders the parasubiculum and receives little piriform input (Fig. 6, injection sites 113DY, 118FB, 124DY). Despite the not insignificant percentage of frontal input to entorhinal areas, the density of labeling in frontal areas resulting from entorhinal injections was relatively low and lowest when the injection was located in the MEA.

The projections from orbital regions arise primarily in layer II. The projections from medial frontal cortex (PL and ILA) arise in layer II and, to a lesser extent, layer V. There is no rostrocaudal topography to the origins of these projections. Layers II, superficial V, and VI provide the input from MOs. Regardless of the subdivision of the

entorhinal cortex, caudal MOs gives rise to a heavier projection.

**Insular areas.** The LEA receives substantially more input from insular cortex than the MEA, 21.2% versus 5.8%. The LEA receives its largest insular input from agranular insular area (4% to 8%) with AIp providing the largest proportion followed by AId and then AIV. The AIp projection originates primarily from layers II and III of all rostrocaudal levels. The AId and AIV projections originate primarily in layer II and to a much lesser extent, in layers III and V of most rostrocaudal levels with the exception of the rostral extreme of the field, which provides little or no LEA input. The granular insular areas, VISC and GU, provide a much smaller input to the LEA, less than 2%. The input from VISC arises primarily from layers II and VI of the caudal portion of the region. Retrogradely labeled cells in the GU were scattered throughout the region and were not confined to any one cell layer. The composition of insular input was similar across all portions of the LEA.

The insular projections to the MEA are weaker, but the relative proportions of input are like those for the LEA. The agranular insular cortex provides 4.7% of the total input to MEA, whereas the granular areas provide only 1.2%. The regional and laminar patterns of origins are similar to those described for LEA with the exception that layer V appears to give rise to the insular-MEA projections. Examination of individual cases indicated that the composition of insular input is also fairly homogeneous for all portions of the MEA except the caudomedial extreme, which appears to receive negligible input from the insular cortex.

**Temporal areas.** The entorhinal cortex receives roughly one-quarter of its cortical input from temporal cortical areas. The perirhinal, postrhinal, and ventral temporal association cortices provide the major temporal input to both the LEA and the MEA. The auditory association cortex provides a more modest input.

The composition of temporal input differs for the LEA and MEA. The LEA receives a comparatively larger proportion, relative to MEA, of input from areas 35 and 36 and a smaller proportion from Te<sub>v</sub> and POR (see Table 2 for percentages). The Te<sub>v</sub> projection to LEA arises from more rostral levels and the Te<sub>v</sub> input to MEA arises caudally. Layers II, superficial V, and deep VI of area Te<sub>v</sub> project to the entorhinal cortex. Based on the percentages of input, area 36 provides a greater proportion of the input to LEA (8.8%) and MEA (5.8%) than does area 35 (6.8% and 1.6%, respectively). Examination of the density data, however, revealed that the density of retrogradely labeled cells in area 35 following an LEA injection was 2.5 times greater than in area 36. For the MEA, the density of labeled cells in area 35 was only slightly greater than in area 36. Projections from area 36 to the entorhinal cortex originate in layers II, superficial V, and VI. Layers II and III of area 35 provide the major entorhinal input, but deeper layers also contribute. The input from POR arises primarily in layers II and III, but superficial layer V and layer VI in the dorsal portion of the region also provide input to the entorhinal cortex.

**Cingulate areas.** The LEA receives only a small proportion (3.1%) of its input from cingulate cortex. RSPd provides the largest input to the LEA, and the projections terminate primarily in the caudal LEA. The MEA receives substantially greater input from cingulate regions (11.2%). Again, the largest input is from retrosplenial cortex,

especially dorsal retrosplenial cortex. The anterior cingulate cortex projects only to the portions of MEA that are near the border with the parasubiculum (Fig. 6, experiments 113DY, 118FB, and 124DY). Otherwise, the projections terminate throughout the MEA. The cingulate-entorhinal projections originate primarily in layer V regardless of the region of origin.

**Parietal areas.** The LEA receives only a small portion of its input from parietal areas, less than 3%. The input arises in layers II, superficial V, and VI of the caudal portions of SSs and PTLp. A very meager input arises in layer VI of caudal SSp. More rostral portions of LEA appear to receive a slightly heavier input from SSs, whereas more caudal portions receive slightly heavier input from PTLp.

The MEA receives substantially more input from parietal areas, about 9%. As is true for the LEA, the parietal input arises in layers II, superficial V, and VI. The more caudal portions of SSs and PTLp provide the stronger input. Most of the parietal input to the MEA terminates in the regions bordering the parasubiculum (Fig. 6, injection sites 113DY, 118FB, 124DY). That portion of the MEA receives 15% of its input from parietal areas, whereas the remaining areas receive less than 3%. Surprisingly, a fairly substantial input to this portion of the MEA arises from caudal SSp. Those projections arise only in layer VI.

**Occipital areas.** Similar to the findings for parietal input to entorhinal cortex, the LEA receives only a meager input from occipital areas. What it does receive originates in layers II and VI of VISm and this terminates in the more caudal portions of LEA.

The MEA receives about 12% of its input from occipital areas. These projections terminate in the caudal regions that border the parasubiculum (Fig. 6, injection sites 113DY, 118FB, 124DY). That portion of the MEA receives 22% of its input from occipital areas, whereas the remaining parts of MEA only receive 2.5%. The major portion of the input to the caudal MEA, about 17%, originates in the visual associational regions, VISl and VISm, primarily in layers II and VI. The remainder originates in layer VI of primary visual cortex, VISp.

### Analysis of control experiments

**Ventral temporal associational injections.** The patterns of labeling resulting from three control injections located dorsal to the dorsal limit of area 36 and at three rostrocaudal locations were also examined (Fig. 6, experiments 109FB, 122FB, and 109DY). As might be expected, there were striking differences in the composition of the inputs to  $Te_v$  associated with the rostrocaudal location of the injection site relative to injections in area 36. Rostral  $Te_v$  receives more somatosensory input, midrostrocaudal levels receive more auditory input, and caudal levels receive more visual and visuospatial input (occipital, posterior parietal, and retrosplenial). Each injection site, however, exhibited a substantially different profile of cortical input than that observed for area 36. In general, the profile of cortical input to  $Te_v$  differs from that of area 36 in the following ways.  $Te_v$  receives negligible input from the piriform cortex. The insular cortex accounts for less than 4% of the input to  $Te_v$ , whereas area 36 receives almost 13% of its input from insular regions. The two areas receive roughly equal amounts of input from temporal regions, although  $Te_v$  receives a greater proportion from auditory areas; 18% of the total input to  $Te_v$  originates in

auditory regions with two-thirds of that from primary auditory cortex. Although both regions receive fairly small proportions of input from cingulate areas, the percentage received by  $Te_v$  is 2.5 times greater than that received by area 36. Area 36 receives more than twice as much entorhinal input as  $Te_v$  and it arises predominantly in LEA.  $Te_v$  receives 2% or 3% of its input from each of the entorhinal subdivisions. Perhaps the greatest difference is that  $Te_v$  receives four times more parietal input than does area 36.  $Te_v$  receives only a slightly greater proportion of input from visual areas than area 36, but substantially more of its visual input arises in primary visual cortex (2.0% for  $Te_v$  as compared to 0.4% for area 36).

**Visual association cortex.** As a control for POR, we examined the distribution of labeling produced by an injection located near the rostral and dorsal border of POR (Fig. 6, experiment 94DY). This injection was located primarily in visual association cortex, VISl (Swanson, 1992), but encroached on the caudal portion of  $Te_v$ .

The profile of cortical input to this portion of VISl differed substantially from those observed following area POR injections. The differences were primarily in the amount of input from temporal, parietal, and occipital areas. VISl receives less total input from temporal areas and over half of that is from POR itself. VISl receives over twice as much input from parietal areas, and this is almost entirely from PTLp. VISl and POR receive roughly equal amounts of input from visual areas, but the projections to VISl originate equally from primary visual cortex and visual association cortex.

### Summary of afferents

**Perirhinal.** Area 36 of the perirhinal cortex receives more higher level cortical input than does area 35. The largest proportion of input, about one-third, arises from the ventral temporal associational area ( $Te_v$ ). Roughly equal amounts (about 10% or 11%) arise in postrhinal and lateral entorhinal areas. In terms of the density of labeling, the projections from POR and  $Te_v$  are about equally heavy.

The predominant inputs to area 35 arise in piriform, entorhinal, and insular cortices. Area 35 receives over one-quarter of its input from the piriform cortex, followed by only slightly less from the lateral entorhinal area. About one-fifth of the total input arises in insular cortices.

**Postrhinal.** The postrhinal cortex receives almost 40% of its input from visual association cortex. The next largest contribution originates in  $Te_v$  followed by the retrosplenial cortex. Other substantial projections arise in area 36 and the posterior parietal cortex. A fairly modest input arises in both subdivisions of the entorhinal cortex and terminates in most portions of the postrhinal cortex, except the dorsal portion. The visual and posterior parietal projections are denser than the retrosplenial and perirhinal inputs.

**Entorhinal.** The complement of inputs, as determined by percentages, is more similar than different for the LEA and MEA. Both receive about one-third of their total input from the piriform cortex. They also receive roughly equal proportions from temporal (20–25%) and frontal (10%) regions. Differences are in the proportions of insular, cingulate, parietal, and occipital input. The LEA receives more input from each insular area than does the MEA for a total of 21.2% as compared to 5.8%. In contrast, the MEA

receives three or four times more input from cingulate, parietal, and occipital regions as compared to the LEA.

Injections in the LEA produced heavier densities of labeling in cortical regions than did injections in the MEA, even though there was no difference between mean volume of injection sites in the two divisions. Although it cannot be assumed that all labeled cells give rise to the same number of terminals in the recipient structure, the density data do suggest that the cortical input to the LEA may be more substantial than the cortical input to the MEA.

## DISCUSSION

The cortical afferents to the perirhinal, postrhinal, and entorhinal cortices were examined using quantitative retrograde tract tracing methods. A limitation of retrograde tract tracing techniques is the possible involvement of fibers of passage. The primary concern with respect to the present findings would be inadvertent involvement of the external capsule or the angular bundle by the injection. Injection sites with any obvious damage to these structures were discarded. One possible exception was noted in Table 1, but the data from that experiment were consistent with other data for the same region. The advantage of having numerous injections in each region is that any eccentricity in a single experiment would likely produce a unique profile of labeling. Thus, "false positive" identification of major cortical afferents using these procedures is unlikely. Another limitation of these quantitative methods is that an assumption must be made that the input to the injection sites reflects the inputs to the entire region. Although injection sites were carefully selected and a relatively large number analyzed for each target region, there were some small gaps, most notably in the most medial portion of the LEA and in the most caudal portion of MEA. It is conceivable, but not likely, that we have missed some cortical inputs that project exclusively to these zones.

Another issue that should be considered is the limitations of the quantitative techniques. A major functional issue is that any interpretation of these data should take into account that assessment of the strength of a projection based on numbers of retrogradely labeled cells (whether in terms of proportions of input to target areas or densities of labeled cells in afferent areas) does not reflect the possible differences in the strength and number of synaptic contacts provided by each retrogradely labeled neuron. The quantitative data reported here, however, will provide important background for investigations of synaptic efficacy and synaptic morphology in these regions.

We elected to report data derived from both proportions of input and densities of labeled cells because each of these measures provides somewhat different information. The density measure contains information about the volume of individual afferent structures as well as the total numbers of labeled cells. In contrast, the proportions are normalized both for volume of afferent regions and for total numbers of labeled cells. The proportions, because they ignore the size of afferent regions and total numbers of labeled cells, permit evaluation of the relative influence of afferent regions upon target regions, thus permitting comparisons of the influence of the various cortical afferent regions. As an example, roughly 10% of the cortical input to both the LEA and the MEA arises in frontal regions. However, the density data demonstrate that twice as many cells per

cubic mm in frontal regions project to the LEA as compared to the MEA. Thus, the information that the frontal projections to LEA are twice as strong as the frontal projections to MEA is available in the density measures. One or the other measure might be more appropriate depending on the issue under evaluation and whether interest is focused on afferent regions or target regions.

## Significance of the findings

The present study revealed that not only are the perirhinal, postrhinal, and entorhinal cortices distinguished by differences in the origins of their cortical afferents, but the subdivisions of the perirhinal and entorhinal cortices also receive proportionately different complements of cortical input. The differences in origins across afferent regions are readily apparent in the graphical presentation in Figure 13A. Area 36 receives substantially more temporal cortical input than does area 35. In contrast, area 35 receives more input from piriform, insular, and entorhinal regions. The most striking difference between the LEA and MEA is the larger proportion of cingulate, parietal, and occipital input received by the MEA.

There are many ways to group cortical afferent regions in order to gain more insight into the data presented in Tables 2 and 3. One useful approach is to examine regional differences in the complements of unimodal and polymodal associational inputs (Table 4 and Fig. 13). Polymodal associational areas provide a larger proportion of input than unimodal associational areas to each region studied (Table 4). Area 36 receives the highest proportion of polysensory input (71.4%) and the MEA receives the lowest (43.1%). Accordingly, area 36 receives the smallest proportion of unimodal input. The small unimodal sensory input to area 36, however, is fairly evenly weighted across all sensory modalities (Table 5 and Fig. 13B). In contrast, area 35 receives one-quarter of its sensory input from piriform cortex and little from other sensory regions. It should be noted that piriform cortex was the only olfactory area quantified, and thus estimates of total olfactory input are not available from these data. The postrhinal cortex receives 60% of its total input from visual and visuospatial areas and only a small percentage from auditory regions. Similar to area 35, the LEA and MEA receive substantial proportions of input from piriform cortex, but there is also a moderate input to the MEA from visual and visuospatial areas.

The comparisons made here concerning the proportions of inputs from various cortical regions do not take into consideration the absolute size of the inputs to different injection sites, i.e., the total number of neurons that were retrogradely labeled following each injection site. The quantitative methods used in the present study actually permit estimates of these numbers. Because there was no difference in the average size of injection sites in each of the target regions, the data indicate that there were consistently more retrogradely labeled cells in the cortex following injections into certain of the cortical areas. The average estimated number of retrogradely labeled neocortical cells per perirhinal cortical injection, for example, was roughly 72,000. A similar number (79,000) was calculated for postrhinal injections, but the number dropped to 47,000 for injections involving the entorhinal cortex. Within the perirhinal cortex, an estimate of 70,000 labeled cells was obtained for injections involving area 36, and 80,000 cells for injections of area 35. The estimates were more

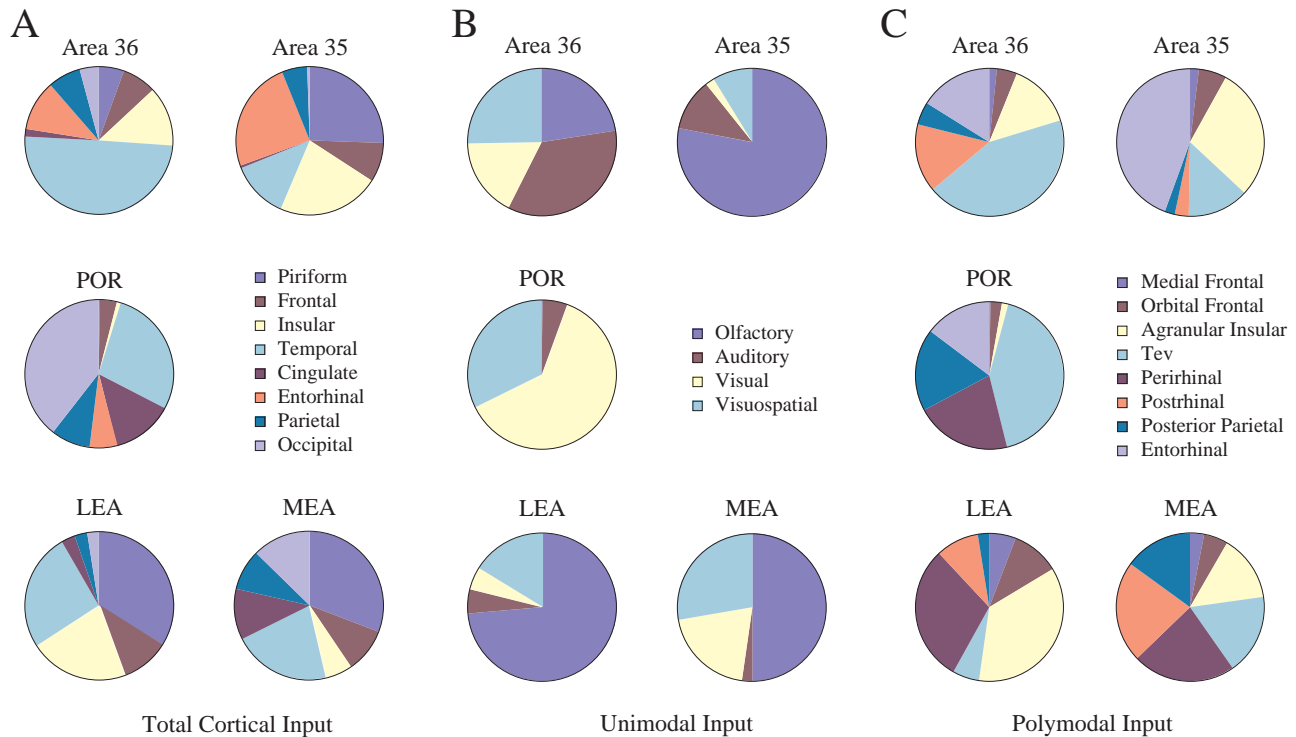


Fig. 13. **A:** Pie charts showing the proportion of total cortical input to each of the five target areas. **B:** Pie charts showing the proportions and sources of polymodal associational input for each of the target areas. **C:** Pie charts showing the proportion of total unimodal input to

each of the five target areas arising from the different sensory cortical regions. LEA, lateral entorhinal area, MEA, medial entorhinal area; Por, postrhinal cortex.

TABLE 4. Percentages of Input to Target Regions by Class of Neocortex<sup>1</sup>

Afferent areas by class of neocortex <sup>2</sup>	Location of injection sites				
	Area 36	Area 35	POR	LEA	MEA
Sensorimotor areas <sup>3</sup>	7.0	8.4	4.1	3.8	11.3
Primary unimodal areas <sup>4</sup>	5.1	1.6	10.0	2.4	4.3
Unimodal associational areas <sup>5</sup>	16.5	34.6	33.4	39.2	41.3
Polymodal associational areas <sup>6</sup>	71.4	55.4	52.5	54.6	43.1

<sup>1</sup>Percentages of input from different classes of neocortex.  
<sup>2</sup>All cortical regions quantified have been placed in one of four classes.  
<sup>3</sup>Includes all MOs, MOp, SSs, and SSP.  
<sup>4</sup>Includes AUD and VISp.  
<sup>5</sup>Includes GU, VISC, Pir, AUDv, VISl, and VISm. Piriform cortex is included with associational regions because it lacks that columnar organization typical of primary sensory cortex.  
<sup>6</sup>Includes all frontal areas except the motor cortex, all agranular insular areas, all temporal areas except auditory cortex, all cingulate areas, both entorhinal subdivisions, and posterior parietal cortex.

TABLE 5. Percentages of Input to Target Regions by Sensory Modality<sup>1</sup>

Afferent areas by sensory modality <sup>2</sup>	Location of injection sites				
	Area 36	Area 35	POR	LEA	MEA
Olfactory areas <sup>3</sup>	5.6	25.6	0.2	33.9	30.7
Gustatory areas <sup>4</sup>	0.5	1.5	0.1	1.1	0.3
Auditory areas <sup>5</sup>	8.8	3.7	3.3	2.4	1.3
Visual areas <sup>6</sup>	4.3	0.6	39.6	2.4	12.4
Visuospatial areas <sup>7</sup>	5.1	1.8	20.2	4.4	16.0

<sup>1</sup>Percentages of input from different unimodal sensory areas and from visuospatial areas.  
<sup>2</sup>See Table 4 for somatosensory input.  
<sup>3</sup>Includes piriform cortex only.  
<sup>4</sup>Includes gustatory insular cortex.  
<sup>5</sup>Includes AUD and AUDv.  
<sup>6</sup>Includes VISp, VISl, and VISm.  
<sup>7</sup>Admittedly, not a sensory modality. Includes cingulate, retrosplenial, and posterior parietal cortices.

disparate for entorhinal subdivisions, 57,000 for the LEA and 33,000 for the MEA. These estimates provide evidence that the magnitude of cortical input in terms of numbers of projecting cells is substantially greater for the perirhinal and postrhinal cortices compared to the entorhinal cortex, especially the MEA.

Figure 14 shows a wiring diagram that summarizes connections based on the densities of retrogradely labeled cells. (Note that the direct projections to the hippocampus were not quantified in the present study and thus are shown in black with no density designation.) These data confirm many of the conclusions that were based on proportions, but reveal certain other facts. It is clear, for example, that the area 35 projections to the LEA are slightly heavier than the reciprocal connections, and that

the postrhinal projection to area 36 is heavier than its reciprocal. The perirhinal-entorhinal connections are much heavier than the postrhinal-entorhinal connections. The wiring diagram also illustrates that visual and visuospatial information reaches the hippocampal formation through robust projections to the postrhinal cortex. The postrhinal cortex then projects directly via modest connections to both subdivisions of the entorhinal cortex, and indirectly through robust projections to the perirhinal cortex. It is also apparent that ventral temporal associational areas project more strongly to area 36 than to the postrhinal cortex, and more strongly to the postrhinal cortex than to area 35. Finally, the wiring diagram illustrates the smaller magnitude of cortical input to the entorhinal cortex, particularly the MEA.

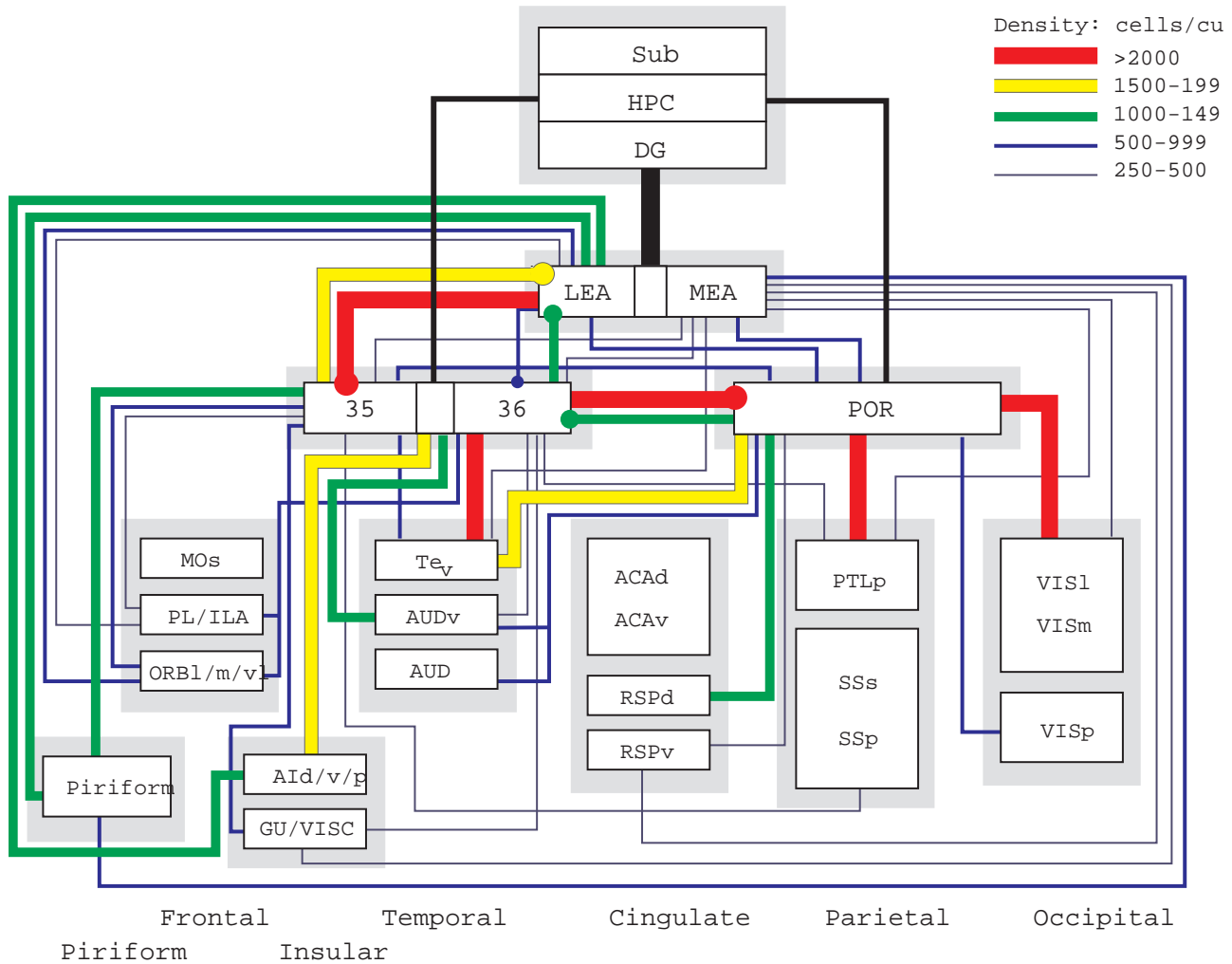


Fig. 14. A wiring diagram representing the pattern and strength of the cortical connectivity of the hippocampal formation (dentate gyrus, DG); hippocampus proper, HPC; subicular complex, sub; and entorhinal cortex, LEA and MEA); the perirhinal cortex (areas 35 and 36); and the postrhinal cortex (POR) for the rat. Strength of connections are based on densities of retrogradely labeled cells in the afferent region as shown in Table 3. Some regions were combined and the density of labeling averaged for simplicity. Reciprocal projections shown were also averaged unless dramatically different. Also for simplicity, the weakest connections ( $< 250$  labeled cells/cu mm) are not shown in the

figure. ACAd and ACAv, dorsal and ventral anterior cingulate cortex; Aid/ v/p, dorsal, ventral, and posterior agranular insular cortices; AUD, primary auditory cortex; AUDv, auditory association cortex; GU, gustatory granular insular cortex; MOs, secondary motor area; Pir, piriform cortex; PTLp, posterior parietal cortex; RSPd,v, retrosplenial cortex, dorsal and ventral; SSp and SSs, primary and supplementary somatosensory areas; Te<sub>v</sub>, ventral temporal cortex; VISC, visceral granular insular cortex; VISl and VISm, lateral and medial visual association cortex; VISp, primary visual cortex.

Figure 14 also highlights the position of the perirhinal and postrhinal cortices as the primary intermediary between the hippocampal formation and the neocortex. A recent study indicated that the perirhinal-entorhinal projection arises preferentially in the relatively small area 35 and terminates preferentially in LEA (Burwell and Amaral, 1998). In the present study, we found that the density of labeled cells in area 35 resulting from LEA retrograde injections was substantially greater than that of any other cortical afferent region. Likewise, the postrhinal projection to the entorhinal cortex terminates preferentially in lateral and caudal portions of the MEA. The density of labeled cells observed in the postrhinal cortex following an injection in the MEA was heavier than that of any other afferent region. Thus, the present study confirms previous

reports that the perirhinal and postrhinal cortices of the rat are an important source of cortical input to the hippocampal formation via their connections with the entorhinal cortex (Burwell and Amaral, 1998; Naber et al., 1997), although, as discussed below, these inputs may be relatively less robust in the rat than they are in the monkey.

### Comparisons with previous studies

The findings reported here confirm and extend previous findings regarding the flow of information through the perirhinal, postrhinal, and entorhinal cortices. In a study of the interconnections of these regions (Burwell and Amaral, 1998), we reported that the postrhinal cortex

projects predominantly to dorsal area 36, that area 35 provides the primary input to the entorhinal cortex, and that the perirhinal-entorhinal projection terminates primarily in the LEA, whereas the postrhinal-entorhinal projection terminates in both the LEA and the MEA (Burwell and Amaral, 1998). The present study confirms those findings using different analytical techniques. The previous study also reported that information is passed from dorsal area 36 to ventral area 36 and ventral area 36 to area 35. The present study extends those findings by documenting the sources and relative strengths of the cortical input to area 36, area 35, and the postrhinal cortex.

Only a single prior study has comprehensively examined the connections of the rat perirhinal cortex (Deacon et al., 1983). That study used tritiated amino acids and horseradish peroxidase methods to examine the cortical afferents of the strip of cortex occupying the fundus and both banks of the posterior half of the rhinal sulcus. According to the cortical boundaries used in the present study, the region examined by Deacon et al. (1983) includes area 35 and the portions of the LEA and MEA that occupy the rhinal sulcus at caudal levels (Dolorfo and Amaral, 1993). The postrhinal cortex, as described here, was not addressed by that study. These differences in boundaries taken into consideration, the present findings are generally consistent with the previous report. Entirely consistent with the present findings, Deacon et al. (1983) reported that the perirhinal cortex receives major projections from medial precentral, prelimbic, ventral lateral orbital, agranular insular, and temporal regions. Differing from the present report, Deacon et al. (1983) also reported major perirhinal input arising from occipital, cingulate, retrosplenial, and parietal regions. Those projections, however, were described as terminating caudally in the perirhinal cortex. Thus, they appear to correspond to projections described here as terminating in the lateral portions of the LEA and MEA, areas that occupy the rhinal sulcus at caudal levels.

The present report is also largely consistent with other prior reports of insular, frontal, olfactory, temporal, and parietal input to perirhinal cortex (reviewed in Burwell et al., 1995). Discrepancies with previous findings are restricted to reports of perirhinal input from retrosplenial and occipital regions. Retrosplenial projections described as terminating in the caudal perirhinal cortex actually appear to terminate in the region defined here as postrhinal cortex (van Groen and Wyss, 1992; Wyss and van Groen, 1992). Likewise, heavy retrograde labeling in visual regions reported to arise from a perirhinal injection site can be explained by the location of the injection, which was primarily in postrhinal cortex (Vaudano et al., 1990). Miller and Vogt (1984) reported visual input to area 36 according to Krieg (1946b), but examination of the pattern of terminal labeling indicated that the input is actually to the postrhinal cortex. Thus, revision of the cortical boundaries of the perirhinal cortex and the definition of the postrhinal cortex appear to account for any inconsistencies with prior reports of perirhinal afferent inputs.

Surprisingly, there are no published comprehensive studies of neocortical input to the rat entorhinal cortex (but for efferents see Insausti et al., 1997; Swanson and Kohler, 1986). The one study that examined the afferent connections of the rat entorhinal cortex using horseradish peroxidase (Beckstead, 1978) reported that the only cortical area found to exhibit abundant retrograde labeling was

the piriform cortex. Although we did observe large numbers of retrogradely labeled cells in the piriform cortex, we found higher densities of labeled cells in area 35 following LEA injections and, as we have reported, many other cortical regions contained retrogradely labeled cells.

### Comparisons with findings in the monkey

In the monkey, substantial sensory information converges onto the entorhinal cortex through its connections with the perirhinal and parahippocampal cortices (Insausti et al., 1987; Jones and Powell, 1970; Suzuki and Amaral, 1994a; Van Hoesen and Pandya, 1972, 1975a,b). The perirhinal cortex receives its predominant input from rostral visual associational areas (Suzuki and Amaral, 1994a). Polymodal associational input to the perirhinal cortex is provided primarily by the parahippocampal cortex. The parahippocampal cortex receives its primary input from caudal visual associational areas as well as visuospatial areas. It receives additional heavy inputs from the retrosplenial cortex and from the polysensory regions located on the dorsal bank of the superior temporal gyrus. The situation is much the same for the rat. Highly processed sensory information converges onto the hippocampus through perirhinal and postrhinal connections via the entorhinal cortex. The heaviest input to the perirhinal cortex originates in ventral temporal associational areas. These areas are polymodal associational cortex, but do receive substantial visual information (reported here, but see also Guldin and Markowitsch, 1983). Additional polymodal input is provided by a heavy postrhinal projection to area 36. As in the monkey, the primary projections to the postrhinal cortex originate in visual and visuospatial areas.

Cross-species differences are most apparent when comparing the details of the unimodal sensory input to these regions. The rat perirhinal, postrhinal, and entorhinal cortices receive a more substantial input from the piriform cortex than is seen for the comparable regions in the monkey (Insausti et al., 1987). In the rat, both the perirhinal and postrhinal cortices receive input from auditory areas, but the auditory input to the perirhinal cortex is stronger. In the monkey, both regions also receive auditory input, but the auditory input to the parahippocampal cortex is stronger (Suzuki and Amaral, 1994a). In the monkey, auditory input to the parahippocampal cortex is restricted to area TH, whereas in the rat the input does not appear to be restricted to any portion of the postrhinal cortex. Finally, the rat perirhinal cortex receives input from all sensory modalities, whereas the monkey perirhinal cortex receives by far its largest unimodal sensory input from the visual system (Suzuki and Amaral, 1994b). The rat postrhinal and the monkey parahippocampal cortices are more similar in that both receive their predominant afferents from visual and visuospatial areas. We have discussed these points elsewhere (Burwell et al., 1995) and proposed that the species differences in the origin of sensory input to these regions may reflect differences in sensory-processing needs.

One apparent difference is in the extent of unimodal inputs to the entorhinal cortex. In the monkey, the only unimodal input to the entorhinal cortex arises in the olfactory bulb and piriform cortex. No other sensory modalities have access to the entorhinal cortex directly (Insausti et al., 1987) but gain entry through the perirhinal, parahippocampal, and other polysensory association cortices (Su-

zuki and Amaral, 1994a). In the rat, direct projections to the entorhinal cortex arise from all sensory modalities, although the input is by far the heaviest from piriform cortex (roughly one-third for both the LEA and the MEA). The LEA receives roughly 5% of its total input from gustatory, auditory, and visual areas. The MEA receives a surprising 12% of its input from visual areas, primarily visual associational areas.

Cross-species differences in the origin of inputs from frontal regions are worth considering in some detail. In the monkey, the inferior convexity of the prefrontal cortex is thought to be involved in visual object working memory, whereas the dorsolateral prefrontal cortex is thought to be preferentially involved in spatial working memory (Wilson et al., 1993). Although the input from the monkey prefrontal cortex to both the perirhinal and the parahippocampal cortex is relatively meager, the perirhinal cortex receives more input from the inferior convexity and the parahippocampal cortex receives more input from dorsolateral prefrontal cortex (Suzuki and Amaral, 1994a). In the rat, Kolb proposed (1984) that the ventral orbital cortex is functionally similar to the primate inferior convexity and orbital regions and that the rat medial frontal cortex (ILA and PL) is functionally similar to the primate dorsolateral prefrontal cortex. Based on findings in the monkey, we might then expect the perirhinal cortex to receive more input from the orbital frontal regions and the postrhinal cortex to receive more input from the medial frontal regions, but this is not the case. The rat perirhinal cortex receives a larger proportion of input from frontal regions than the postrhinal cortex, but both the perirhinal and postrhinal cortices receive more input from the orbital than from the medial frontal regions. Although the medial frontal cortex in the rat has been implicated in spatial functions (Aggleton et al., 1995; Kesner et al., 1989) and it has been proposed that the rat medial frontal cortex (ILA and PL) is functionally similar to the primate dorsolateral prefrontal cortex (Kolb, 1984), on connective grounds, it appears that the ILA and PL are more similar to the monkey prelimbic frontal regions, areas 25 and 32 (Barbas and Pandya, 1989; Preuss and Goldman-Rakic, 1991). The findings reported here suggest that medial frontal regions in the rat are more similar to the monkey medial frontal cortex than dorsolateral prefrontal cortex, but this issue warrants further examination. Another important species difference is that the monkey perirhinal and parahippocampal cortices do not receive any motor input (Suzuki and Amaral, 1994a), whereas the rat perirhinal and postrhinal cortices receive 2–3% of their input from the secondary motor cortex and a smaller amount from the primary motor cortex.

Perhaps the most striking similarity between the connections of the perirhinal, parahippocampal, and entorhinal regions in the rat and monkey is in the organization of connections among visuospatial regions. In both species, the retrosplenial cortex provides a prominent input to the parahippocampal cortex that is considerably stronger than the input from cingulate cortex (this study and Suzuki and Amaral, 1994a). In the rat, the retrosplenial cortex also projects prominently to the portion of the MEA that is preferentially innervated by postrhinal cortex (Burwell and Amaral, 1998). As in the rat, the monkey retrosplenial cortex projects to the caudal half of the entorhinal cortex (Insausti et al., 1987), the portion that receives the heaviest parahippocampal input (Suzuki and Amaral, 1994b).

The rat postrhinal, but not the perirhinal, cortex receives substantial input from posterior parietal cortex. Similarly, the posterior parietal projection to the parahippocampal cortex in the monkey is well-established (Cavada and Goldman-Rakic, 1989; Jones and Powell, 1970), but the perirhinal cortex receives little or no input from there (Suzuki and Amaral, 1994a). Finally, as is true with the retrosplenial connections, the posterior parietal cortex preferentially targets the MEA of the rat entorhinal cortex (this study) and the caudal entorhinal cortex of the monkey (Insausti et al., 1987). Thus, in the rat and the monkey, visuospatial information is redundantly provided to the medial entorhinal region (caudal in the monkey) by parallel pathways, i.e., directly from the posterior parietal and retrosplenial cortices and indirectly via their connections with the postrhinal/parahippocampal cortex.

Other important similarities and differences are apparent in the perirhinal, postrhinal, and entorhinal interconnections. In the monkey, the parahippocampal cortex provides a stronger input to the perirhinal cortex than the reciprocal projection (Suzuki and Amaral, 1994b) and the rat postrhinal cortex provides a stronger input to area 36 than does the reciprocal projection. By comparison, the area 35–postrhinal interconnections are more modest and equal in strength. Regarding the projections to the entorhinal cortex, the topographies are somewhat similar. In both species, the perirhinal cortex projects preferentially to rostromedial entorhinal areas and the postrhinal/parahippocampal cortex projects preferentially to caudomedial areas. However, the projections are weighted differently. In the monkey, the perirhinal and parahippocampal projections to the entorhinal cortex are similar in strength. In the rat, the perirhinal projections to the entorhinal cortex are stronger than the postrhinal ones. Moreover, in the monkey, the perirhinal/parahippocampal to entorhinal projections are comparable in strength to the return projections. In the rat, except for the area 35–LEA connections, the return projections are relatively less substantial. The area 35–LEA reciprocal connections, however, are equal in strength.

Much has been made in recent years of the information that the perirhinal and parahippocampal cortices provide a major portion of the input to the monkey entorhinal cortex. The present study allows comparison of the situation in the rat and monkey. Our findings indicate that the perirhinal cortex gives rise to only 15.6% of the input to the LEA and 7.1% of the input to the MEA. The postrhinal cortex gives rise to 4.9% and 7.1% of the input to the LEA and MEA, respectively. Thus, the perirhinal/post-rhinal input to the entorhinal cortex accounts for roughly 15–20% or the total input. This is in dramatic contrast to the situation in the monkey where over two-thirds of the cortical input to the monkey entorhinal cortex arises from the perirhinal and parahippocampal cortices (Insausti et al., 1987). Even if the numbers for the rat are recomputed excluding the comparatively large piriform input, the perirhinal/post-rhinal input still accounts for only about one-third of the total input. This is consistent with an interpretation that the origins of the cortical afferents to these regions appear to be more distributed in the rat than they are in the monkey. Another example of this principle is that no region within the rat perirhinal or postrhinal cortex receives on average more than 50% of its input from temporal areas, whereas in the monkey, the perirhinal cortex receives 95% of its input from the temporal lobe and

the parahippocampal cortex receives 67–74%, depending on the subdivision (Suzuki and Amaral, 1994a).

### Functional implications

Evidence in the rat and the monkey indicates that the perirhinal cortex plays a substantive role for certain forms of memory (Herzog and Otto, 1997; Meunier et al., 1993; Ramus et al., 1994; Rosen et al., 1992; Wiig et al., 1997; Wiig and Bilkey, 1994), but a function for the parahippocampal cortex has yet to be clearly identified. The perirhinal cortex, but not the parahippocampal cortex, appears to contribute to visual recognition memory for objects (Ramus et al., 1994). There is also evidence that neurons in these two cortical regions differ in their electrophysiological responses. Unlike perirhinal neurons, parahippocampal neurons do not differentiate between presentation of novel and familiar stimuli (Fahy et al., 1993). Monkeys with lesions of the perirhinal cortex or parahippocampal cortex exhibit different patterns of impairment on a two-choice spatial discrimination task followed by spatial reversal (Teng et al., 1997). Thus, it appears that the perirhinal and postrhinal/parahippocampal cortices have different functions, a conclusion that is consistent with the connectional differences between these regions in both the rat and the monkey (for the rat, present findings and Burwell and Amaral, 1998; for the monkey Suzuki and Amaral, 1994a,b).

The rat postrhinal cortex and the monkey parahippocampal cortex are closely connected with cortical regions thought to be involved in the processing of visual and spatial information, suggesting that these regions themselves may contribute to visuospatial functions. The emerging evidence from studies in the monkey is consistent with this view. In the aforementioned Teng et al. study (1997), the deficit associated with parahippocampal lesions was in the spatial reversal task, but not in initial learning of the spatial discrimination. Malkova and Mishkin (1997) reported that aspiration lesions of the parahippocampal cortex resulted in impairment on an object-place association task. Rolls and O'Mara (1995) described cells localized in the monkey parahippocampal cortex and hippocampus that fired in response to visual input and depended on where the monkey was looking in the environment. In human imaging studies, activity in the parahippocampal gyrus is associated with spatial working memory (Courtney et al., 1996) and with learning and recall of topographic information (Aquirre et al., 1996). Thus, based on the anatomical connections and preliminary findings in human and nonhuman primates, it is reasonable to hypothesize that the postrhinal/parahippocampal region is involved in the processing of visuospatial information.

The neuroanatomy of the postrhinal/parahippocampal cortices also suggests certain other possibilities for cognitive functions. The posterior parietal cortex in the rat is defined by its connectivity with thalamic input from the lateral posterior nucleus (Reep et al., 1994). The lateral posterior nucleus, which is considered the homologue of the pulvinar in the monkey (Price, 1995), provides a prominent input to the postrhinal cortex (Burwell et al., 1995). This pattern of connections for the postrhinal cortex in the rat parallels interconnections among the pulvinar, parahippocampal cortex, and visuospatial processing areas in monkeys (Baleydier and Mauguier, 1985). It has been proposed that the posterior parietal cortex functions to disengage attention, whereas the pulvinar may mediate

shifting and focusing of attention (reviewed in Desimone and Duncan, 1995). The close anatomical association of these regions with the postrhinal/parahippocampal cortex suggests an attentional role for that region in visuospatial functions.

### CONCLUSIONS

We have found that the origin of cortical input differs for the perirhinal, postrhinal, and entorhinal cortices. Although the perirhinal and postrhinal cortices provide substantial input to the entorhinal cortex, the topography of those and other entorhinal inputs suggests that entorhinal functions are not entirely dependent on perirhinal/ postrhinal input. Likewise, the cortical afferents of the perirhinal and postrhinal cortices are consistent with physiological and neuropsychological findings indicating that these regions may have unique cognitive functions that are at least partially independent of their interactions with the hippocampal formation. The challenge of determining the specific contributions of the entorhinal, perirhinal and postrhinal/parahippocampal cortices to memory and other cognitive functions remains an important area for future research in the rat and nonhuman primate.

### ACKNOWLEDGMENTS

The authors gratefully acknowledge the technical support of Dan Antoniello and Guadalupe Garcia. We also thank Wendy A. Suzuki for comments on an earlier version of this manuscript and Peter R. Rapp for assistance in designing the quantitative analyses. This research was supported in part by NIH grant NS 16980 to D.G.A., and an NIMH postdoctoral fellowship (F32-NS09247) to R.D.B.

### LITERATURE CITED

- Aggleton, J.P., N. Neave, S. Nagle, and A. Sahgal (1995) A comparison of the effects of medial prefrontal, cingulate cortex, and cingulum bundle lesions on tests of spatial memory: Evidence of a double dissociation between frontal and cingulum bundle contributions. *J. Neurosci.* 15: 7270–7281.
- Amaral, D.G. and J.L. Price (1983) An air pressure system for the injection of tracer substances into the brain. *J. Neurosci. Methods* 9:35–43.
- Amaral, D.G., R. Insausti, and W.M. Cowan (1987) The entorhinal cortex of the monkey: I. Cytoarchitectonic organization. *J. Comp. Neurol.* 264: 326–355.
- Aquirre, G.K., J.A. Detre, D.C. Alsop, and M. D'Esposito (1996) The parahippocampus subserved topographical learning in man. *Cereb. Cortex* 6:823–829.
- Arnault, P. and M. Roger (1990) Ventral temporal cortex in the rat: Connections of secondary auditory areas Te2 and Te3. *J. Comp. Neurol.* 302:110–123.
- Baleydier, C. and F. Mauguier (1985) Anatomical evidence for medial pulvinar connections with the posterior cingulate cortex, the retrosplenial area, and the posterior parahippocampal gyrus in monkeys. *J. Comp. Neurol.* 232:219–228.
- Barbas, H. and D.N. Pandya (1989) Architecture and intrinsic connections of the prefrontal cortex in the Rhesus monkey. *J. Comp. Neurol.* 286:353–375.
- Beckstead, R.M. (1976) Convergent thalamic and mesencephalic projections to the anterior medial cortex in the rat. *J. Comp. Neurol.* 166:403–416.
- Beckstead, R.M. (1978) Afferent connections of the entorhinal area in the rat as demonstrated by retrograde cell-labeling with horseradish peroxidase. *Brain Res.* 152:249–264.
- Blackstad, T.W. (1956) Commissural connections of the hippocampal region in the rat, with special reference to their mode of termination. *J. Comp. Neurol.* 105:417–537.

- Brodman, K. (1909) Vergleichende Lokalisationslehre der Grosshirnrinde in ihren Prinzipien dargestellt auf Grund des Zellenbaues. Leipzig: Barth.
- Buckley, M.J. and D. Gaffan (1997) Impairment of visual object-discrimination learning after perirhinal cortex ablation. *Behav. Neurosci.* *111*:467–475.
- Burwell, R.D. and D.G. Amaral (1995) The issue of parahippocampal cortex in the rat. *Society for Neuroscience Abstracts* *21*:1494.
- Burwell, R.D. and D.G. Amaral (1998) The perirhinal and postrhinal cortices of the rat: Interconnectivity and connections with the entorhinal cortex. *J. Comp. Neurol.* *391*:293–321.
- Burwell, R.D., M.P. Witter, and D.G. Amaral (1995) The perirhinal and postrhinal cortices of the rat: A review of the neuroanatomical literature and comparison with findings from the monkey brain. *Hippocampus* *5*:390–408.
- Cavada, C. and P.S. Goldman-Rakic (1989) Posterior parietal cortex in rhesus monkey: I. Parcellation of areas based on distinctive limbic and sensory corticocortical connections. *J. Comp. Neurol.* *287*:393–421.
- Chandler, H.C., V. King, J.V. Corwin, and R.L. Reep (1992) Thalamocortical connections of the posterior parietal cortex. *Neurosci. Lett.* *143*:237–242.
- Chapin, J.K. and C.S. Lin (1984) Mapping the body representation in the SI cortex of anesthetized and awake rats. *J. Comp. Neurol.* *229*:199–213.
- Courtney, S.M., L.G. Ungerleider, K. Keil, and J.V. Haxby (1996) Object and spatial visual working memory activate separate neural systems in human cortex. *Cereb. Cortex* *6*:39–49.
- Deacon, T.W., H. Eichenbaum, P. Rosenberg, and K.W. Eckmann (1983) Afferent connections of the perirhinal cortex in the rat. *J. Comp. Neurol.* *220*:168–190.
- Desimone, R. and J. Duncan (1995) Neural mechanisms of visual attention. *Ann. Rev. Neurosci.* *18*:193–222.
- Dolorfo, C.L. and D.G. Amaral (1993) Connectional and immunocytochemical differences at the border of the entorhinal and perirhinal cortices in the rat. *Soc. Neurosci. Abst.* *19*:853.
- Dolorfo, C.L. and D.G. Amaral (1998) The entorhinal cortex of the rat: Topographic organization of the cells of origin of the perforant path projection to the dentate gyrus. *J. Comp. Neurol.* (in press).
- Donoghue, J.P. and S.P. Wise (1982) The motor cortex of the rat: Cytoarchitecture and microstimulation mapping. *J. Comp. Neurol.* *212*:76–88.
- Fahy, F.L., I.P. Riches, and M.P. Brown (1993) Neuronal activity related to visual recognition memory: Long-term memory and the encoding of recency and familiarity information in the primate anterior and middle inferior temporal and rhinal cortex. *Exp. Brain Res.* *96*:457–472.
- Guldin, W.O. and H.J. Markowitsch (1983) Cortical and thalamic afferent connections of the insular and adjacent cortex of the rat. *J. Comp. Neurol.* *215*:135–153.
- Gundersen, H.J.G., P. Bagger, T.F. Bendtsen, S.M. Evans, L. Korbo, N. Marcussen, A. Møller, K. Nielsen, J.R. Nyengaard, B. Pakkenberg, F.B. Sørensen, A. Vesterby, and M.J. West (1988) The new stereological tools: Disector, fractionator, nucleator and point sampled intercepts and their use in pathological research and diagnosis. *APMIS* *96*:857–881.
- Haberly, L.B. and J.L. Price (1978) Association and commissural fiber systems of the olfactory cortex in the rat. I. Systems originating in the piriform cortex and adjacent areas. *J. Comp. Neurol.* *178*:711–740.
- Habib, M. and A. Sirigu (1987) Pure topographical disorientation: A definition and anatomical basis. *Cortex* *23*:73–85.
- Herzog, C. and T. Otto (1997) Odor-guided fear conditioning in rats: 2. Lesions of the anterior perirhinal cortex disrupt fear conditioned to the explicit conditioned stimulus but not to the training context. *J. Neurosci.* *11*:1265–1272.
- Hughes, H.C. (1977) Anatomical and neurobehavioral investigations concerning the thalamo-cortical organization of the visual system. *J. Comp. Neurol.* *175*:311–336.
- Hunt, M.E., R.P. Kesner, and R.B. Evans (1994) Memory for spatial locations: Functional dissociation of entorhinal cortex and hippocampus. *Psychobiology* *22*:186–194.
- Insausti, R., D.G. Amaral, and M.W. Cowan (1987) The entorhinal cortex of the monkey: II. Cortical afferents. *J. Comp. Neurol.* *264*:356–395.
- Insausti, R., M.T. Herrero, and M.P. Witter (1997) Entorhinal cortex of the rat: Cytoarchitectonic subdivisions and the origin and distribution of cortical efferents. *Hippocampus* *7*:146–183.
- Jones, E.G. and T.P.S. Powell (1970) An anatomical study of converging sensory pathways within the cerebral cortex of the monkey. *Brain* *93*:793–820.
- Kesner, R.P., G. Farnsworth, and B.V. DiMattia (1989) Double dissociation of egocentric and allocentric space following medial prefrontal and parietal cortex lesions in the rat. *Behav. Neurosci.* *103*:956–961.
- Kolb, B. (1984) Functions of the frontal cortex of the rat: A comparative review. *Brain Res. Rev.* *8*:65–98.
- Kreig, W.J.S. (1946a) Connections of the cerebral cortex. I. The albino rat. A. Topography of the cortical areas. *J. Comp. Neurol.* *84*:221–275.
- Kreig, W.J.S. (1946b) Connections of the cerebral cortex. I. The albino rat. B. Structure of the cortical areas. *J. Comp. Neurol.* *84*:277–323.
- Krettek, J.E. and J.L. Price (1977) The cortical projections of the mediodorsal nucleus and adjacent thalamic nuclei in the rat. *J. Comp. Neurol.* *171*:157–192.
- Leonard, B.W., D.G. Amaral, L.R. Squire, and S. Zola-Morgan (1995) Transient memory impairment in monkeys with bilateral lesions of the entorhinal cortex. *J. Neurosci.* *15*:5637–5659.
- Malkova, L. and M. Mishkin (1997) Memory for the location of objects after separate lesions of the hippocampus and parahippocampal cortex in the Rhesus monkey. *Soc. Neurosci. Abst.* *23*:12.
- Meunier, M., J. Bachevalier, M. Mishkin, and E.A. Murray (1993) Effects on visual recognition of combined and separate ablations of the entorhinal and perirhinal cortex in Rhesus monkeys. *J. Neurosci.* *13*:5418–5432.
- Miller, M.W. and B.A. Vogt (1984) Direct connections of rat visual cortex with sensory, motor, and association cortices. *J. Comp. Neurol.* *226*:184–202.
- Myhrer, T. and K. Wangen (1996) Marked retrograde and anterograde amnesia of a visual discrimination task in rats with selective lesions of the perirhinal cortex. *Neurobiol. Learn. Mem.* *65*:244–252.
- Naber, P.A., M. Caballero-Bleda, B. Jorritsma-Byham, and M.P. Witter (1997) Parallel input to the hippocampal memory system through peri- and postrhinal cortices. *NeuroReport* *8*:2617–2621.
- Otto, T., F. Schottler, U. Staubli, H. Eichenbaum, and G. Lynch (1991) Hippocampus and olfactory discrimination learning: Effects of entorhinal cortex lesions on olfactory learning and memory in a successive-cue, go-no-go task. *Behav. Neurosci.* *105*:111–119.
- Paxinos, G. and C. Watson (1986) *The Rat Brain in Stereotaxic Coordinates*. Second ed. San Diego: Academic Press.
- Paxinos, G. and C. Watson (1997) *The Rat Brain in Stereotaxic Coordinates*. Third ed. San Diego: Academic Press.
- Preuss, T.M. and P.S. Goldman-Rakic (1991) Myelo- and cytoarchitecture of the granular frontal cortex and surrounding regions in the strepsirrhine primate *Galago* and the anthropoid primate *Macaca*. *J. Comp. Neurol.* *310*:429–474.
- Price, J.L. (1995) Thalamus. In G. Paxinos (ed): *The Rat Nervous System*. Second ed. San Diego: Academic Press, pp. 629–648.
- Ramus, S.J., S. Zola-Morgan, and L.R. Squire (1994) Effects of lesions of perirhinal cortex or parahippocampal cortex on memory in monkeys. *Soc. Neurosci. Abst.* *20*:1074.
- Reep, R.L., H.C. Chandler, V. King, and J.V. Corwin (1994) Rat posterior parietal cortex: Topography of corticocortical and thalamic connections. *Exp. Brain Res.* *100*:67–84.
- Rolls, E.T. and S.M. O'Mara (1995) View-responsive neurons in the primate hippocampal complex. *Hippocampus* *5*:409–424.
- Rose, M. (1929) *Cytoarchitektonischer atlas der grobhirnrinde der maus*. *J. Psychol. Neurol.* *40*:1–32.
- Rosen, J.B., J.M. Hitchcock, M.J.D. Miserendino, W.A. Falls, S. Campeau, and M. Davis (1992) Lesions of the perirhinal cortex but not of the frontal, medial prefrontal, visual, or insular cortex block fear-potentiated startle using a visual conditioned stimulus. *J. Neurosci.* *12*:4624–4633.
- Sanderson, K.J., W. Welker, and G.M. Shambes (1984) Reevaluation of motor cortex and sensorimotor overlap in the cerebral cortex of albino rats. *Brain Res.* *292*:251–260.
- Schmued, L.C. and J.H. Fallon (1986) Fluoro-Gold: A new fluorescent retrograde axonal tracer with numerous unique properties. *Brain Res.* *377*:147–154.
- Scoville, W.B. and B. Milner (1957) Loss of recent memory after bilateral hippocampal lesions. *J. Neurol. Neurosurg. Psychiatry* *20*:11–21.
- Suzuki, W.A. and D.G. Amaral (1994a) The perirhinal and parahippocampal cortices of the Macaque monkey: Cortical afferents. *J. Comp. Neurol.* *350*:497–533.
- Suzuki, W.A. and D.G. Amaral (1994b) Topographic organization of the reciprocal connections between the monkey entorhinal cortex and the perirhinal and parahippocampal cortices. *J. Neurosci.* *14*:1856–1877.
- Swanson, L.W. (1992) *Brain Maps: Structure of the Rat Brain*. Amsterdam: Elsevier.

- Swanson, L.W. and C. Kohler (1986) Anatomical evidence for direct projections from the entorhinal area to the entire cortical mantle in the rat. *J. Neurosci.* *6*:3010–3023.
- Teng, E., L.R. Squire, and S. Zola (1997) Different memory roles for the parahippocampal and perirhinal cortices in spatial reversal. *Soc. Neurosci. Abst.* *23*:12.
- van Groen, T. and J.M. Wyss (1992) Connections of the retrosplenial dysgranular cortex in the rat. *J. Comp. Neurol.* *315*:200–216.
- Van Hoesen, G.W. and D.N. Pandya (1972) Cortical afferents to the entorhinal cortex of the Rhesus monkey. *Science* *175*:1471–1473.
- Van Hoesen, G.W. and D.N. Pandya (1975a) Some connections of the entorhinal (area 28) and perirhinal (area 35) cortices of the rhesus monkey. I. Temporal lobe afferents. *Brain Res.* *95*:1–24.
- Van Hoesen, G.W. and D.N. Pandya (1975b) Some connections of the entorhinal (area 28) and perirhinal (area 35) cortices of the Rhesus monkey. II. Frontal lobe afferents. *Brain Res.* *95*:25–38.
- Vaudano, E., C.R. Legg, and M. Glickstein (1990) Afferent and efferent connections of temporal association cortex in the rat: A horseradish peroxidase study. *Eur. J. Neurosci.* *3*:317–330.
- Vogt, B.A. (1985) Cingulate cortex. In A. Peters and E.G. Jones (eds): *Cerebral Cortex, Volume 4, Association and Auditory Cortices*. New York and London: Plenum Press, pp. 89–179.
- Vogt, B.A. and M.W. Miller (1983) Cortical connections between rat cingulate cortex and visual, motor, and postsubicular cortices. *J. Comp. Neurol.* *216*:192–210.
- Vogt, B.A. and A. Peters (1981) Form and distribution of neurons in rat cingulate cortex: Areas 32, 24, and 29. *J. Comp. Neurol.* *195*:603–625.
- West, M.J. (1993) New stereological methods for counting neurons. *Neurobiol. Aging* *14*:275–285.
- Wiig, K.A. and D.K. Bilkey (1994) The effects of perirhinal cortical lesions on spatial reference memory in the rat. *Behav. Brain Res.* *63*:101–109.
- Wiig, K.A., M.F. Bear, and R.D. Burwell (1997) Comparable memory impairment following electrolytic and neurotoxic lesions of the perirhinal cortex. *Soc. Neurosci. Abst.* *23*:1599.
- Wiig, K.A., L.N. Cooper, and M.F. Bear (1996) Temporally graded retrograde amnesia following separate and combined lesions of the perirhinal cortex and fornix in the rat. *Learn. Mem.* *3*:313–325.
- Wilson, F.A.W., S.P.O. Scaldie, and P.S. Goldman-Rakic (1993) Dissociation of object and spatial processing domains in primate frontal cortex. *Science* *260*:1955–1958.
- Witter, M.P. and D.G. Amaral (1991) Entorhinal cortex of the monkey: V. Projections to the dentate gyrus, hippocampus, and subicular complex. *J. Comp. Neurol.* *307*:437–459.
- Witter, M.P., H.J. Groenewegen, F.H. Lopes de Silva, and A.H.M. Lohman (1989) Functional organization of the extrinsic and intrinsic circuitry of the parahippocampal region. *Prog. Neurobiol.* *33*:161–253.
- Wyss, J.M. and T. van Groen (1992) Connections between the retrosplenial cortex and the hippocampal formation in the rat: A Review. *Hippocampus* *2*:1–12.